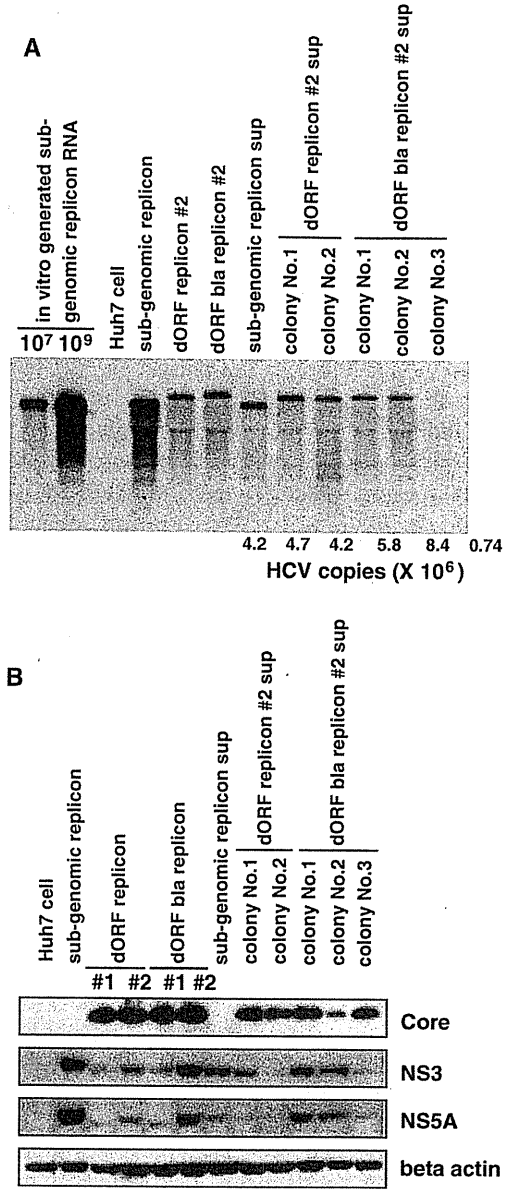

Fig. 5 Northern blot analysis of colonies formed after infection. 10^7, 10^9: amounts of in vitro-generated subgenomic replicon RNA loaded. Numbers below the lanes are the HCV copy number per μg of total RNA (A). Huh-7 cells, subgenomic replicon cells, dORF replicon cell #2, dORF bla replicon cell #2, subgenomic replicon sup: colony from cells transduced with subgenomic replicon supernatant, colony No.1, 2 of dORF replicon #2 sup: colonies from cells infected with dORF replicon #2 supernatant, colony No.1, 2, and 3 of dORF bla replicon #2 sup: colonies from cells infected with dORF bla replicon #2 supernatant. Western blot analysis of colonies formed after infection (B). The order of the lanes is identical to that for the northern blot, except for the dORF and dORF bla replicons, which represent two clones in this figure

clones of the same dORF replicon cells, which may have been due to the accumulation of different mutations in the structural region, although we have not yet confirmed this

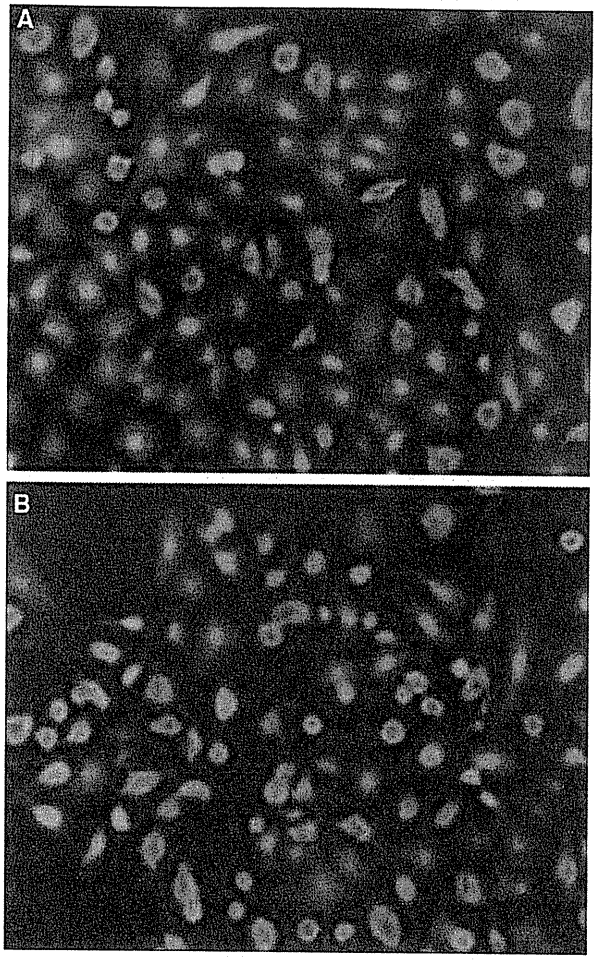

Fig. 6 Detection of beta-lactamase activity in dORF replicon cells. Parental dORF bla replicon #2 cell (A) and colony no. 3 cloned from cells infected with dORF bla replicon #2 cell supernatant (B). Blue fluorescence shows high beta-lactamase activity, indicating that the reporter gene functioned normally after infection

hypothesis. We also observed colonies being formed by cells that were treated with supernatant containing subgenomic replicons, and these colonies most likely represent the so-called "non-specific transduction" of the subgenomic replicon. Although this dORF supernatant infection could be blocked by the anti-CD81 antibody reported previously [30], we cannot exclude the possibility that the infection we observed was due to highly efficient "non-specific transduction," as we could not determine whether "non-specific transduction" also could be affected by the anti-CD81 antibody because of the low colony-forming ability of the supernatant of subgenomic replicons.

We also demonstrated that the reporter gene that was inserted in addition to the neomycin resistance gene could be transmitted to the new generation of viruses. This finding raises the possibility of producing sufficient amounts of reporter virus constitutively.

In summary, we established an infectious-particle-producing HCV replicon system. This achievement should yield more precise information about the encapsidation signal of HCV, which was kept intact despite the partitioning of the genome. This system also allows analysis of the pathway of HCV infection, including adsorption of virions to cell-surface receptors, penetration, uncoating, virus particle assembly, and HCV release. Moreover, the dORF replicon system may be used as a convenient tool to investigate the utility of the newly established siRNA system [14, 27] and evaluation of compounds that are effective against subgenomic replicons.

Although we believe that the reason for our success is our new construct, further examination is necessary to verify our findings.

Materials and methods

Construction and RNA transcription

To construct dORF replicon RNA, the second half of the NS2 region of the HCV-R6 strain [25] was replaced in frame with the foot and mouth disease virus (FMDV) 2A protease gene, the neomycin resistance gene, and the encephalomyocarditis virus (EMCV) internal ribosomal entry site (IRES). In addition, the region from NS3 to the beginning of NS5B was replaced with the 1bneo/delS replicon sequence from the N strain of genotype 1b [6](kindly provided by Dr. Seeger). This construct was designated as the "divided open reading frame carrying full genome" (dORF) replicon. The subgenomic replicon construct was also prepared from the R6 strain and also contained the 1bneo/delS replacement. For the reporter assay, the FMDV 2A protease gene and beta-lactamase gene (bla; Invitrogen) were inserted after the remaining NS2 gene to produce the dORF bla replicon construct. Replication-deficient versions of these three replicons were also prepared by deleting 27 nucleotides, including the GDD motif of NS5B polymerase.

In vitro transcription of these replicon RNAs was performed using the MEGAscript kit (Ambion).

Cell culture and electroporation

Huh-7 cells were cultured in DMEM (SIGMA) with 10% fetal bovine serum. Replicon cells were maintained in the same medium supplemented with 300 μg/mL G418 (Invitrogen). These cells were passaged 3 times a week at a 4:1 splitting ratio. Electroporation of replicon RNA was performed as described previously [17]. The subgenomic replicon (1bneo/delS replicon) cells were treated with 1000 IU of IFN-α for 2 months and cloned by the limited dilution method. Two of these clones were designated as HCV replicon-cured Huh-7 cells F2 and K4. The cell line containing the full-genome replicon of genotype1b, namely the NNC#2 clone [15], was a kind gift from Dr. Shimotohno of Keio University.

Northern blot analysis and quantification of HCV RNA

Total RNA was purified from cells using ISOGEN (Nippon Gene) for northern blot analysis or ABI prizm6100 (Applied Biosystems) for real-time RT-PCR. Purified RNAs were quantified by absorbance at 260 nm. For northern blot analysis, 30 μg of each total RNA was used with a Northern Max Kit (Ambion) according to the manufacturer's instructions. The probe for detection of HCV RNA was a PCR fragment of the NS5B region (nucleotide numbers 7629–7963) that had been biotin-labeled using a BrightStar Psoralen-Biotin Kit (Ambion) according to the manufacturer's instructions. Following hybridization of the membranes, the probe was detected using a BrightStar BioDetect Kit (Ambion) according to the manufacturer's instructions, and luminescence was detected using the LAS1000 detection system (Fujifilm). Measurement of the HCV RNA copy number by real-time RT-PCR was performed using an ABI PRISM 7900 system (Applied Biosystems) as described previously [24].

Western blot analysis

Western blot analysis was carried out using the conventional semi-dry blot method. Cells were lysed with buffer containing 100 mM Tris-HCl (pH 7.4) and 4% sodium dodecyl sulfate. A 10-μg amount of protein from each sample was separated by SDS-PAGE through a 4–20% gradient gel (Invitrogen) and transferred to the membrane according to the gel manufacturer's protocol. The antibodies used in this study were anti-core mouse monoclonal antibody (MAb), anti-E1 MAb, anti-E2 MAb (reported previously; [25]), anti-NS3 antiserum (reported previously; [25]), anti-NS5B antiserum (Upstate), and anti-beta-actin MAb (Abcam). Horseradish peroxidase-labeled anti-mouse and anti-rabbit IgG goat antibodies (Santa Cruz Biotechnology and DAKO, respectively) were used as the secondary antibody. The membranes were treated using an ECL Plus kit (Amersham) according to the manufacturer's instructions, and luminescence was detected using an LAS1000 system (Fujifilm).

Density gradient analysis and core ELISA

Culture supernatants from replicon cells were loaded onto 10–60% sucrose density gradient tubes with or without 10-fold concentration in an Amicon-100 (Millipore). The

tubes were then ultracentrifuged at 100,000 *g* for 16 h and fractionated. NP-40 was added to the culture supernatants to a final concentration of 0.5%, and they were then incubated at 4°C for 30 min. For electron microscopy, the culture supernatant was concentrated, loaded onto a 60% sucrose cushion, and ultracentrifuged at 100,000 *g* for 4 h. The interface between the concentrated medium and the sucrose cushion was collected and separated by the density gradient method described above. A 2-mL fraction from 5 ml to 7 mL from the bottom, with a density of 1.1–1.2 g/mL, was examined by electron microscopy after further concentration by the sucrose cushion ultracentrifugation method described above. The amount of core protein in the fractions was quantified using an Ohso ELISA kit in accordance with the manufacturer's instructions.

Electron microscopy

The concentrated fraction of core protein was observed by scanning and transmission electron microscopy. For scanning electron microscopy, the sample was allowed to settle on the surface of a poly-L-lysine-coated glass cover slip for 30 min, and the attached sample was then fixed with 0.1% glutaraldehyde in 0.1 M phosphate buffer (pH 7.4) for 10 min, washed three times with 0.1 M phosphate buffer, and post-fixed with 1% osmium tetroxide in the same buffer for 10 min. After dehydration through a graded series of ethanol, the samples were dried in a freeze dryer (Hitachi ES-2020, Hitachi) using t-butyl alcohol, coated with osmium tetroxide, approximately 2 nm thick, using an osmium plasma coater (NL-OPC80; Nippon Laser and Electronics Laboratory), and then examined using a Hitachi S-4800 field emission scanning electron microscope at an accelerating voltage of 10 kV [23]. For transmission electron microscopy, the sample was allowed to settle on a formvar-coated nickel grid for 10 min, dried in air, incubated with rabbit anti-E2RR6 antibody (prepared as described in the supplementary information), washed with PBS, and then incubated with goat anti-rabbit IgG coupled to 10-nm colloidal gold (British BioCell). After negative staining with 2% uranyl acetate, the sample was examined using a JEM 1200EX transmission electron microscope (JEOL) at an accelerating voltage of 80 kV.

Rabbit anti-E2 RR6 antibody to the HCV-E2 protein was prepared as follows: The E2 gene of HCV type 1b [25] was cloned under the control of the ATI-P7.5 hybrid promoter of vaccinia virus vector pSFB4 and allowed to recombine with the Lister strain of the vaccinia virus to give vector RVV. Rabbits were infected intradermally with 10^8 p.f.u. of RVV, and 2 months later, they received two booster injections with the purified E2 protein. HCV-E2 protein was expressed from the RVV vector and purified by lentil lectin column chromatography and affinity chromatography using an anti-E2 monoclonal antibody [25].

Infection

A 2.5-ml aliquot of cleared culture supernatants from replicon cells was added to approximately 70% confluent of Huh-7 cells in 25-cm^2 flasks, and the same amount of complete DMEM was added 2 h later. Infected cells were transferred to 75-cm^2 flasks the next day and to four 10-cm dishes 2 days later. G418 at a concentration of 300 μg/mL was added to the medium immediately after the second passage. The three types of Huh-7 cells used in this study included the one purchased from J.C.R.B. and the 2 IFN-cured replicon cell lines F2 and K4 described above. The medium was changed every other day. For the blocking experiment, cells were treated with the anti-CD81antibody as described previously [30]. Cells were fixed with 10% formalin/PBS(-) for 10 min after washing with PBS(-) and staining with 1% crystal violet/PBS(-) for 1 h before washing with water.

Beta-lactamase detection assay

Beta-lactamase activity was detected using a GeneBLAzer In Vivo Detection Kit (Invitrogen) according to the manufacturer's instructions and observed using a fluorescence microscope (Nikon) with UV light excitation.

Acknowledgments The authors would like to thank Dr. Christoph Seeger of the Fox Chase Cancer Center for providing the 1bneo/delS replicon plasmid and Dr. Kunitada Shimotohno of Keio University for providing full-genome genotype 1b replicon clone NNC#2. We also thank Etsuko Endo for her secretarial work and Dr. Masahiro Shuda for fruitful discussions. This study was supported in part by grants from the Ministry of Education, Culture, Sports, Science and Technology of Japan, the Program for Promotion of Fundamental Studies in Health Sciences of the National Institute of Biomedical Innovation of Japan, and the Ministry of Health, Labour and Welfare of Japan.

References

1. Blight KJ, McKeating JA and Rice CM (2002) Highly permissive cell lines for subgenomic and genomic hepatitis C virus RNA replication. J Virol 76:13001-13014
2. Choo QL, Kuo G, Weiner AJ, Overby LR, Bradley DW and Houghton M (1989) Isolation of a cDNA clone derived from a blood-borne non-A, non-B viral hepatitis genome. Science 244:359-362
3. Date T, Kato T, Miyamoto M, Zhao Z, Yasui K, Mizokami M and Wakita T (2004) Genotype 2a hepatitis C virus subgenomic

replicon can replicate in HepG2 and IMY-N9 cells. J Biol Chem 279:22371-6
4. Date T, Miyamoto M, Kato T, Morikawa K, Murayama A, Akazawa D, Tanabe J, Sone S, Mizokami M and Wakita T (2007) An infectious and selectable full-genome replicon system with hepatitis C virus JFH-1 strain. Hepatol Res 37:433-443
5. Frolova E, Frolov I and Schlesinger S (1997) Packaging signals in alphaviruses. J Virol 71:248-258
6. Guo J, Bichko VV and Seeger C (2001) Effect of alpha interferon on the hepatitis C virus replicon. J Virol 75:8516-8523
7. Ikeda M, Yi M, Li K and Lemon SM (2002) Selectable subgenomic and genome-length dicistronic RNAs derived from an infectious molecular clone of the HCV-N strain of hepatitis C virus replicate efficiently in cultured Huh7 cells. J Virol 76:2997-3006
8. Jia X-Y, Van Eden M, Busch MG, Ehrenfeld E and Summers DF (1998) Trans-encapsidation of a poliovirus replicon by different picornavirus capsid proteins. J Virol 72:7972-7977
9. Johansen LK and Morrow CD (2000) The RNA encompassing the internal ribosome entry site in the poliovirus 5′ nontranslated region enhances the encapsidation of genomic RNA. Virology 273:391-399
10. Kanda T, Basu A, Steele R, Wakita T, Ryerse JS, Ray R and Ray RB (2006) Generation of infectious hepatitis C virus in immortalized human hepatocytes. J Virol 80:4633-4639
11. Kanto T, Hayashi N, Takehara T, Hagiwara H, Mita E, Naito M, Kasahara, A, Fusamoto H and Kamada T (1994) Buoyant density of hepatitis C virus recovered from infected hosts: two different features in sucrose equilibrium density-gradient centrifugation related to degree of liver inflammation. Hepatology 19:296-302
12. Kato T, Furusaka A, Miyamoto M, Date T, Yasui K, Hiramoto J, Nagayama K, Tanaka T and Wakita T (2001) Sequence analysis of hepatitis C virus isolated from a fulminant hepatitis patient. J Med Virol 64:334-339
13. Kato T, Date T, Miyamoto M, Furusaka A, Tokushige K, Mizokami M and Wakita, T (2003) Efficient replication of the genotype 2a hepatitis C virus subgenomic replicon. Gastroenterology 125:1808-1817.
14. Kim M, Shin D, Kim SI and Park M (2006) Inhibition of hepatitis C virus gene expression by small interfering RNAs using a tricistronic full-length viral replicon and a transient mouse model. Virus Res 122:1-10
15. Kishine H, Sugiyama K, Hijikata M, Kato N, Takahashi H, Noshi T, Nio Y, Hosaka M, Miyanari Y, Shimotohno K (2002) Subgenomic replicon derived from a cell line infected with the hepatitis C virus. Biochem Biophys Res Commun 293:993-9
16. Lindenbach BD, Evans MJ, Syder AJ, Wolk B, Tellinghuisen TL, Liu C C, Maruyama T, Hynes RO, Burton DR, McKeating JA and Rice CM (2005) Complete replication of hepatitis C virus in cell culture. Science 309:623-626
17. Lohmann V, Korner F, Koch J, Herian U, Theilmann L and Bartenschlager R (1999) Replication of subgenomic hepatitis C virus RNAs in a hepatoma cell line. Science 285:110-113
18. Lu, HH, Alexander L and Winner E (1995) Construction and genetic analysis if dicistronic Polioviruses containing open reading frames for epitopes of Human Immunodeficiency Virus type 1 gp120. J Virol 69:4797-4806
19. Mattion NM, Reilly PA, DiMichele SJ, Crowley JC and Weeks-Levy C (1994) Attenuated poliovirus strain as a live vector: expression of regions of rotavirus outer capsid protein VP7 by using recombinant Sabin 3 viruses. J Virol 68:3925-3933
20. Pietschmann T, Lohmann V, Kaul A, Krieger N, Rinck G, Rutter G, Strand D and Bartenschlager R (2002) Persistent and transient replication of full-length hepatitis C virus genomes in cell culture. J Virol 76:4008-4021
21. Pietschmann T, Kaul A, Koutsoudakis G, Shavinskaya A, Kallis S, Steinmann E, Abid K, Negro F, Dreux M, Cosset FL and Bartenschlager R (2006) Construction and characterization of infectious intragenotypic and intergenotypic hepatitis C virus chimeras. Proc Natl Acad Sci USA 103:7408-7413
22. Pileri P, Uematsu Y, Campagnoli S, Galli G, Falugi F, Petracca R, Weiner AJ, Houghton M, Rosa D, Grandi G and Abrignani S (1998) Binding of hepatitis C virus to CD81. Science 282:938-941
23. Suzuki H, Murasaki K, Kodama K and Takayama H (2003) Intracellular localization of glycoprotein VI in human platelets and its surface expression upon activation. Bri J Haematol 121:904-912
24. Takeuchi T, Katsume A, Tanaka T, Abe A, Inoue K, Tsukiyama-Kohara K, Kawaguchi R, Tanaka S and Kohara M (1999) Real-time detection system for quantification of hepatitis C virus genome. Gastroenterology 116:636-42
25. Tsukiyama-Kohara K, Tone S, Maruyama I, Inoue K, Katsume A, Nuriya H, Ohmori H, Ohkawa J, Taira K, Hoshikawa Y, Shibasaki F, Reth M, Minatogawa Y and Kohara M (2004) Activation of the CKI-CDK-Rb-E2F pathway in full genome hepatitis C virus-expressing cells. J Biol Chem 279:14531-14541
26. Wakita T, Pietschmann T, Kato T, Date T, Miyamoto M, Zhao Z, Murthy K, Habermann A, Krausslich HG, Mizokami M, Bartenschlager R and Liang TJ (2005) Production of infectious hepatitis C virus in tissue culture from a cloned viral genome. Nat Med 11:791-796
27. Watanabe T, Sudoh M, Miyagishi M, Akashi H, Arai M, Inoue K, Taira K, Yoshiba M and Kohara M (2006) Intracellular-diced dsRNA has enhanced efficacy for silencing HCV RNA and overcomes variation in the viral genotype. Gene Ther 13:883-92
28. Yi MK and Lemon SM (2004) Adaptive mutations producing efficient replication of genotype 1a Hepatitis C virus RNA in normal Huh7 cells. J Virol 78:7904-7915
29. Yi MK, Villanueva RA, Thomas D, Wakita T and Lemon SM (2006) Production of infectious genotype 1a hepatitis C virus (Hutchinson strain) in cultured human hepatoma cells. Proc Natl Acad Sci USA 103:2310-2315
30. Zhong J, Gastaminza P, Cheng G, Kapadia S, Kato T, Burton DR, Wieland SF, Uprichard SL, Wakita T and Chisari FV (2005) Robust hepatitis C virus infection in vitro. Proc Natl Acad Sci USA 102:9294-9299

Journal of Medical Virology 83:801–809 (2011)

Translocase of Outer Mitochondrial Membrane 70 Expression Is Induced by Hepatitis C Virus and Is Related to the Apoptotic Response

Takashi Takano,[1,2,3] Michinori Kohara,[2] Yuri Kasama,[1] Tomohiro Nishimura,[1,4] Makoto Saito,[1] Chieko Kai,[3] and Kyoko Tsukiyama-Kohara[1]*

[1]*Faculty of Life Sciences, Department of Experimental Phylaxiology, Kumamoto University, Kumamoto, Japan*
[2]*Department of Microbiology and Cell Biology, Tokyo Metropolitan Institute of Medical Science, Tokyo, Japan*
[3]*Laboratory Animal Research Center, Institute of Medical Science, The University of Tokyo, Tokyo, Japan*
[4]*The Chemo-Sero-Therapeutic Research Institute, Kikuchi Research Center, Kyokushi, Kikuchi, Kumamoto, Japan*

The localization of hepatitis C virus (HCV) proteins in cells leads to several problems. The translocase of outer mitochondrial membrane 70 (TOM70) is a mitochondrial import receptor. In this study, TOM70 expression was induced by HCV infection. TOM70 overexpression induced resistance to tumor necrosis factor-alpha (TNF-α)-mediated apoptosis but not to Fas-induced apoptosis in HepG2 cells. TOM70 was found to be induced by the HCV non-structural protein (NS)3/4A protein, and silencing of TOM70 decreased the levels of the NS3 and Mcl-1 proteins. These results indicate that TOM70 can directly interact with the NS3 protein. In hepatoma cells, silencing of TOM70 induced apoptosis and increased caspase-3/7 activity but did not modify caspase-8 and caspase-9 activity. TOM70 silencing-induced apoptosis was impaired in HCV NS3/4A protein-expressing cells. Thus, this study revealed a novel finding, that is, TOM70 is linked with the NS3 protein and the apoptotic response. ***J. Med. Virol. 83:801–809, 2011.***

KEY WORDS: hepatitis C virus; translocase of outer mitochondrial membrane 70; apoptosis; non-structural protein 3; tumor necrosis factor-alpha

INTRODUCTION

Hepatitis C virus (HCV) infection causes acute and chronic hepatitis, cirrhosis, and hepatocellular carcinoma (HCC) [Seeff, 2002]. HCV easily establishes chronic infection, and localization of HCV proteins is reported to induce several disturbances in cells. One of the major target organelles of HCV is the mitochondrion, and HCV non-structural protein (NS)3/4A protease cleaves the mitochondrial antiviral signaling (MAVS)/IPS-1/VISA/Cardif protein, thereby impairing interferon signaling [Li et al., 2005] and influencing apoptotic responses [Nomura-Takigawa et al., 2006; Deng et al., 2008; Lei et al., 2009].

Most mitochondrial proteins are synthesized in the cytosol as preproteins, targeted to the mitochondria by cytosolic factors such as HSP70 and mitochondrial import stimulation factor (MSF), and transported to the intramitochondrial compartments by the preprotein import machineries of the outer and inner membranes (TOM and TIM complexes, respectively) [Mihara and Omura, 1996; Schatz, 1996; Neupert, 1997; Pfanner and Meijer, 1997]. The TOM machinery consists of two import receptors, namely, TOM20 and TOM70, and several other subunits that are arranged in a tightly bound complex termed the general import pore [Pfanner and Geissler, 2001; Hoogenraad et al., 2002; Stojanovski et al., 2003]. TOM70 was identified in *Saccharomyces cerevisiae* as a 70-kDa protein with no known function [Truscott et al., 2001]. TOM70 is recognized as the primary receptor for proteins with internal targeting signals, such as the F_1-ATPase β-subunit

Additional Supporting Information may be found in the online version of this article.

Grant sponsor: Ministry of Health and Welfare of Japan; Grant sponsor: Clinical and Epidemiological Studies of Emerging and Re-emerging Infectious Diseases (Cooperative Research Project).

Takashi Takano present address is Division of Veterinary Public Health, Nippon Veterinary and Life Science University, 1-7-1 Kyonan, Musashino, Tokyo 180-8602, Japan.

*Correspondence to: Kyoko Tsukiyama-Kohara, Faculty of Life Sciences, Department of Experimental Phylaxiology, Kumamoto University, 1-1-1 Honjo, Kumamoto 860-8556, Japan.
E-mail: kkohara@kumamoto-u.ac.jp

Accepted 13 December 2010
DOI 10.1002/jmv.22046
Published online in Wiley Online Library (wileyonlinelibrary.com).

and cytochrome c_1 [Truscott et al., 2001]. TOM70 interacts with human myeloid cell leukemia-1 (Mcl-1), a Bcl-2 family member, and this interaction facilitates the mitochondrial targeting of Mcl-1 [Chou et al., 2006]. Mcl-1 can interact with the HCV core protein and suppresses core-induced apoptosis [Mohd-Ismail et al., 2009].

In the present study, it was found that TOM70 activity was enhanced by HCV. This study addresses TOM70 modification by HCV and its role in the apoptotic response.

MATERIALS AND METHODS

Cells

WRL68, HepG2, HuH-7, and HepG2 cells expressing non-structural proteins (Lenti-NS3/4A-HepG2, Lenti-NS4B-HepG2, Lenti-NS5A-HepG2, Lenti-NS5B-HepG2, and Lenti-empty-HepG2) were maintained and established as described previously [Tsukiyama-Kohara et al., 2004; Nishimura et al., 2009; Saitou et al., 2009]. The Cre/loxP conditional expression system for full-length HCV cDNA (*HCR6-Rz*) in RzM6 cells [Tsukiyama-Kohara et al., 2004] was induced using 100 nM of 4-hydroxytamoxifen (Sigma–Aldrich, St. Louis, MO) and passaged for 8 days (RzM6-8d) or for more than 44 days (RzM6-LC) [Nishimura et al., 2009] (Supplementary Fig. 1). Cell viability was measured using WST-8 (Dojindo, Kumamoto, Japan).

Purification and Matrix-Assisted Laser Desorption Ionization Time-of-Flight Mass Spectrometry (MALDI-TOF-MS) Analysis of p70 and TOM70 Expression Vector

p70 was identified using MALDI-TOF-MS. The p70 band was excised, alkylated using 40 mM iodoacetamide/0.1 M NH_4HCO_3, and digested using trypsin. The p70 peptides were purified using an UltiMate capillary high-performance liquid chromatography system (Dionex) and analyzed using a 4700 Proteomics Analyzer (Applied Biosystems, Foster City, CA), as described previously [Jensen et al., 1999]. An expression vector with myc and His tags was constructed for TOM70 as follows: Total RNA was isolated from HuH-7 cells (10^6) by using the ISOGEN reagent (Nippon Gene, Tokyo, Japan). Purified RNA (2 μg) was reverse transcribed using SuperScriptIII (Invitrogen, Carlsbad, CA) and oligo$(dT)_{12-18}$ primer (Invitrogen), according to the manufacturer's protocol. The coding region of TOM70 cDNA was amplified by polymerase chain reaction (PCR) with LA *Taq* polymerase (Takara Bio, Shiga, Japan) and TOM70-F2 (5′-GGATCCGCAGAGGACACTTGTCATGGC-3′), which contained a *Bam*HI restriction site (underlined), as the forward primer and TOM70-R2 (5′-GCTGGAGTGCAGTGGCTATTC-3′) as the reverse primer. The amplified TOM70 cDNA was subcloned into the pCR2.1-TOPO vector. *Bam*HI–*Eco*RI-digested TOM70 cDNA was subcloned into pcDNA6/Myc-His(+) (Invitrogen) (TOM70-pcDNA6).

Immunoprecipitation (IP) and Western Blotting (WB)

The cells were solubilized in lysis buffer (20 mM HEPES-NaOH [pH 7.5], 1 mM EDTA [pH 7.5], 1 mM dithiothreitol, 1 μM diisopropylfluorophosphate, 150 mM NaCl, and 1% TritonX-100). Samples were centrifuged at 20,400*g* for 10 min at 4°C, and the supernatants were used for IP. Protein-G sepharose 4B beads (GE Healthcare, Piscataway, NJ; 20 μl) were washed, mixed with 2-243a antibody (2 μg) in 1% BSA-phosphate-buffered saline (PBS), and placed on a rotary shaker at 4°C for 1 hr. Next, the beads were washed three times with lysis buffer and treated with the cell lysate (4°C, overnight). The IP mix was washed four times with lysis buffer and solubilized with 2× SDS sample buffer (150 mM Tris [pH 6.8], 4% SDS, 20% glycerol, 10% 2-mercaptoethanol, and 0.2% bromophenol blue). WB was performed as described previously [Nishimura et al., 2009]. Anti-myc monoclonal antibody (mAb) (9E10; Santa Cruz Biotechnology, Santa Cruz, CA), anti-HCV core mouse mAb (31-2), and anti-NS3 rabbit polyclonal antibody (R212) were used to examine the interaction between NS3 and myc-TOM70. Anti-Mcl-1 antibody (S-19; Santa Cruz Biotechnology) and anti-MAVS antibody (ab25084; ChIP grade; Abcam, Cambridge, MA) were also used. Professor Mihara (Kyusyu University) kindly provided anti-rat TOM70 polyclonal antibody (rTOM70).

Immunofluorescence Assay (IFA)

For mitochondrial staining, MitoRed (Dojindo) was added to the cell culture medium and incubated for 1 hr. The cells were fixed in 4% paraformaldehyde. The slides were then washed with PBS, permeabilized with 1% Triton X-100; and reacted with 2-243a mAb (1 μg/ml) and a polyclonal antibody against the endoplasmic reticulum (ER) (anti-PDI; 1:1,000; Stressgen Bioreagent, Kampenhout, Belgium) in 0.025% Tween-20 PBS, followed by reaction with FITC-conjugated goat anti-mouse IgG mAb (1:1,000; Cappel Products, Portland, ME) and Alexa 568-conjugated goat anti-rabbit IgG $(Fab')_2$ fragment (Invitrogen) in 0.025% Tween-20 PBS. The slides were covered with Vector Shield (Vector Laboratories, Burlingame, CA) and observed under an Olympus Fluoview laser-scanning microscope (Olympus, Tokyo, Japan).

Evaluation of Cell Death by Assessing Fas or Tumor Necrosis Factor (TNF)-α

The cells were plated in a 96-well plate (10^4 cells/well; Becton Dickinson, Franklin Lake, NJ) and transfected with empty pcDNA6 or TOM70-pcDNA6 (40 ng/well) by using the Lipofectamine 2000 reagent (Invitrogen). After 48 hr, the cells were treated with anti-Fas

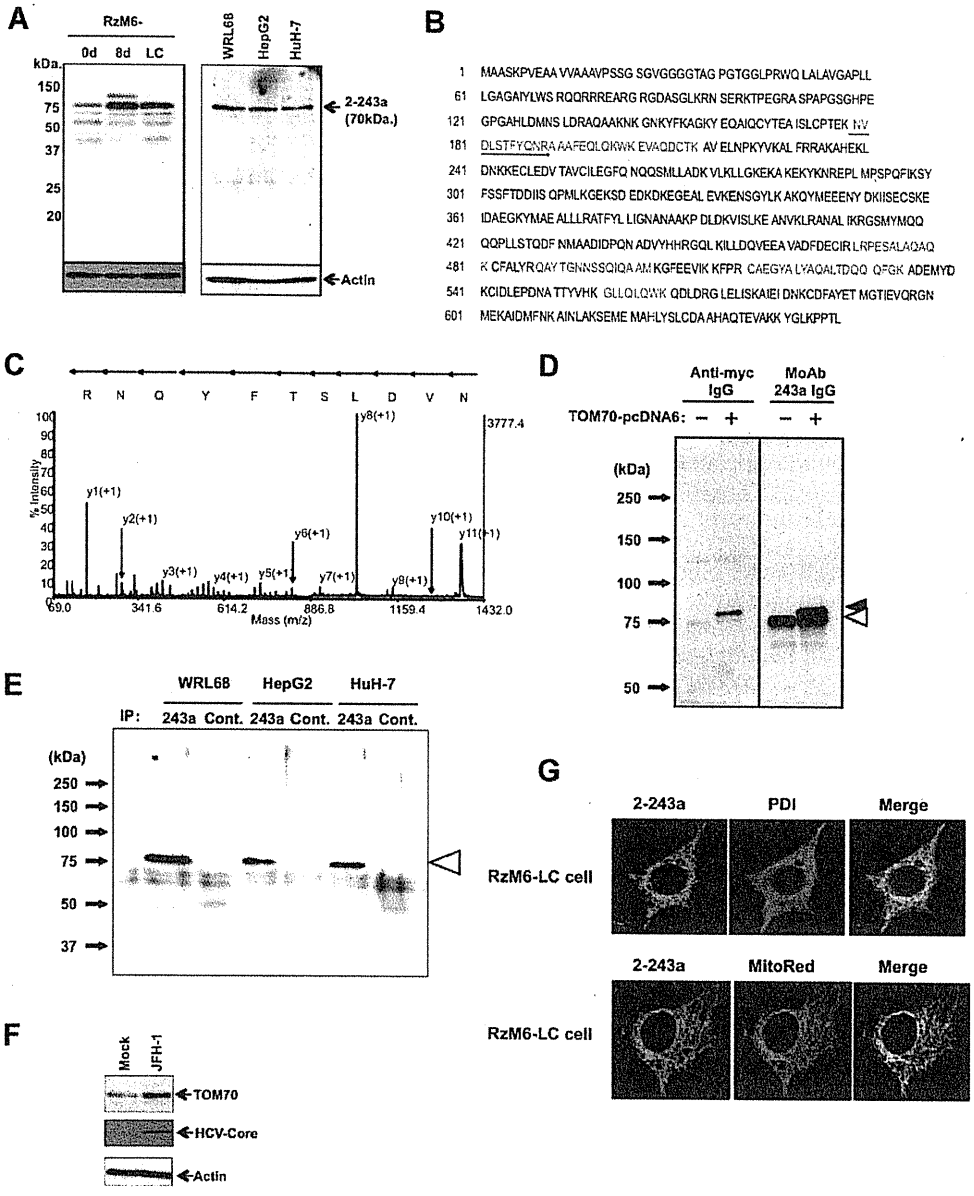

Fig. 1. TOM70 is induced by HCV and is localized in the mitochondria. **A**: TOM70 induction was examined by WB in RzM6-8d and RzM6-LC days (left panel), and TOM70 expression was compared in WRL68, HepG2, and HuH-7 cells (right panel). **B**: Identification of p70 by MALDI-TOF-MS analysis. The sequence of peptides in the amino acid sequence of TOM70 protein was determined using MALDI-TOF-MS analysis (red characters). **C**: MS/MS spectra of the peptide NVDLSTFYQNR (149–159). The sequence covers 14% of the amino acid sequence of TOM70. **D**: Identification of p70 by IP-WB. Expression of TOM70-pcDNA6 in HuH-7. Cell lysates were examined using WB with mAb 2-243a or the anti-myc antibody. myc-TOM70-pcDNA6 expression was recognized by both mAb 2-243a and the anti-myc antibody (black triangle). The expression of cellular TOM70 (empty triangle) was recognized only by mAb 2-243a. **E**: Cell lysates were immunoprecipitated with anti-rat TOM70 antibody and analyzed using WB with mAb 2-243a. The empty triangle indicates TOM70. The molecular weight markers are shown on the left. **F**: Expression of TOM70 and the core protein in mock- and HCV JFH-1-infected HuH-7 cells. **G**: Localization of TOM70 in RzM6-LC cells. The cells were stained with mAb 2-243a and polyclonal antibody against PDI or MitoRed. The magnification is 800×.

antibody (CH-11; 0–20 ng/ml; Beckman Coulter, Murmasaka) or recombinant human TNF-α (0–100 ng/ml; PeproTech, Rocky Hill, NJ), followed by addition of cycloheximide (CHX; 10 μg/ml). After treatment for 24 hr, apoptotic cell death was evaluated by determining cell viability with the WST-8 reagent. Next, the terminal deoxynucleotidyl transferase dUTP nick-end labeling (TUNEL) assay was performed using the TMR red in situ cell death detection kit (Roche, Basel, Switzerland).

Generation of Small Interfering Ribonucleic Acid (siRNA) for TOM70

siRNAs for two regions of TOM70, namely, TOM70-d1-siRNA (primer set: TOM70-dicer1-F and TOM70-dicer1-R) and TOM70-d2-siRNA (primer set: TOM70-dicer2-F and TOM70-dicer2-R) were generated.

Gene-specific dsDNA for TOM70 was constructed by PCR using TOM70-pcDNA6 as the template. TOM70-dicer1-F (5′-GCGTAATACGACTCACTATAGGGAGATGTTTGGCCTTTAAGTATCC-3′) was used as the forward primer, and TOM70-dicer1-R (5′-GCGTAATACGACTCACTATAGGGAGATGATATCATCCGTGAAAGAAC-3′) was used as the reverse primer; both primers contained a T7 promoter sequence (underlined). PCR performed using these primers yielded a 434-bp product. PCR with the forward primer TOM70-dicer2-F (5′-GCGTAATACGACTCACTATAGGGAGAATGTTTGCATTGTACCGCC-3′) and the reverse primer TOM70-dicer2-R2 (5′-GCGTAATACGACTCACTATAGGGAGATTTGCAACTTCTGTCTGGGC-3′), both of which contained a T7 promoter sequence (underlined), yielded a 474-bp product. Luciferase was amplified from pGL3-Basic (Takara Bio) with Luci-dicer2-F (5′-GCGTAATACGACTCACTATAGGGAGACGGTTTTGGAATGTTTACTAC-3′) as the forward primer and Luci-dicer2-R (5′-GCGTAATACGACTCACTATAGGGAGAGCTGATGTAGTCTCAGTGAGC-3′), as the reverse primer, yielding a 309-bp product; both primers contained a T7 promoter sequence (underlined). LA *Taq* polymerase was used for the PCR. All PCR products were analyzed by agarose electrophoresis before purification with the Wizard SV Gel and PCR Clean-Up System (Promega, Madison, WI).

In vitro transcription was performed with the Dicer siRNA generation kit (Genlantis, San Diego, CA), according to the manufacturer's instructions. Briefly, in vitro transcription reactions were performed in a 20-μl volume with 1 μg PCR product as the template; the reaction mixture was incubated at 37°C for 4 hr, followed by purification with the reagents provided in the Dicer siRNA generation kit. The dsDNA (20 μl) obtained was finally in a 100-μl volume after incubation at 37°C for 27 hr. The siRNAs obtained were purified and quantified according to the manufacturer's instructions.

Next, the cells were plated in 24- or 96-well plates (BD Bioscience, Sparks, MD) at a density of 5×10^4 or 10^4 cells/well, respectively, and left overnight for adherence. The siRNAs (14 nM) generated were transfected to cells by using Lipofectamine RNAiMAX (Invitrogen) and Opti-MEM (Invitrogen). The cells were characterized 48 hr after transfection.

Caspase Assay

The activities of caspase-3/7, caspase-8, and caspase-9 were measured on the basis of the cleavage of a proluminescent substrate containing the DEVD sequence, by using the commercially available Caspase-Glo 9 Assay, Caspase-Glo 8 Assay, and Caspase-Glo 3/7 Assay kits (Promega) and a luminometer (Aloka, Tokyo, Japan). Caspase activity was quantified according to the manufacturer's instructions.

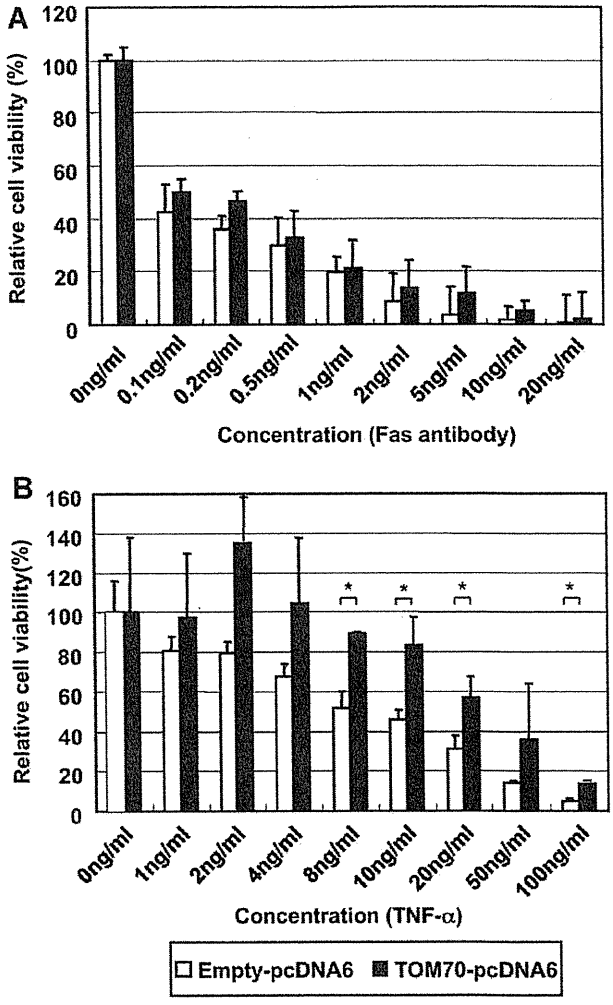

Fig. 2. TOM70 overexpression induced TNF-α-mediated apoptotic resistance. TOM70 overexpression affected TNF-α-mediated apoptosis but not Fas-mediated apoptosis. Cells were transfected with empty pcDNA6 (white bar) or TOM70-pcDNA6 (black bar). After 48 hr, they were treated with (**A**) Fas antibody (0–20 ng/ml) or (**B**) TNF-α (0–100 ng/ml). After 24 hr, cell viability was measured using WST-8. A,B: The data represent the average of the values obtained from triplicate experiments, and the vertical bars indicate the SD. $^*P < 0.05$ (two-tailed Student's *t*-test).

Statistical Analysis

Data were analyzed for statistical significance by using the Student's *t*-test. *P*-values lower than 0.05 were considered statistically significant.

RESULTS

Identification of the p70 Molecule and Induction by HCV

mAbs against RzM6-LC cells were screened, and the clone 2-243a, which recognizes p70, was obtained

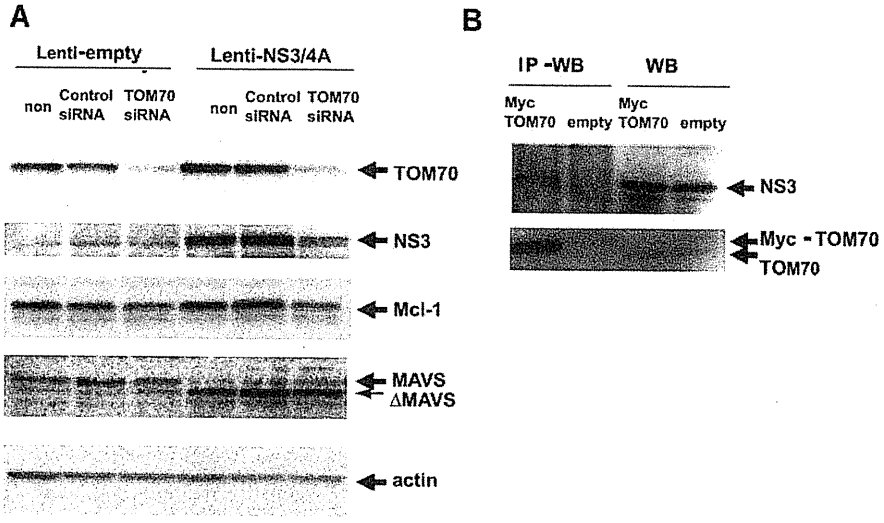

Fig. 3. Interaction between TOM70 and NS3 protein. **A**: The effect of TOM70 siRNA in cells transfected with empty or NS3/4A-containing lentivirus vectors was examined by WB with mAb 2-243a for TOM70; anti-NS3 rabbit polyclonal antibody; anti-Mcl-1 rabbit polyclonal antibody; anti-MAVS rabbit polyclonal antibody; and anti-actin antibody. **B**: The interaction between TOM70 and NS3 was assessed using IP-WB. NS3-expressing HepG2 cells were transfected with pcDNA6-TOM70 (mycTOM70) or pcDNA6 alone (empty) and immunoprecipitated with the anti-myc antibody (9E10). NS3 was detected using polyclonal rabbit anti-NS3 antibody (upper image), and TOM70 was detected using mAb 2-243a (lower image).

(Fig. 1A). p70 was induced to a greater extent by HCV expression after 8 days (RzM6-8d) or more than 44 days (RzM6-LC) than before HCV expression (RzM6-0d). The p70 expression level did not differ among the human hepatic cell lines (WRL68, HepG2, and HuH-7) (Fig. 1A, right panel). p70 was characterized (Fig. 1B–E): The sequence of peptides determined using MALDI-TOF-MS (Fig. 1B) and the MS/MS spectra of the p70 peptide sequence NVDLSTFYQNR (Fig. 1C) are provided. TOM70-pcDNA6 expression in HuH-7 cells was detected by WB with mAb 2-243a (Fig. 1D). Cell lysates were immunoprecipitated with anti-rat TOM70 antibody and detected by WB using mAb 2-243a (Fig. 1E). These results indicate that mAb 2-243a recognizes TOM70. Next, the effect of HCV infection on TOM70 expression was examined (Fig. 1F), and infection with the HCV JFH-1 strain [Wakita et al., 2005] induced TOM70 expression in HuH-7 cells (Fig. 1F). TOM70 localization was characterized using an indirect fluorescence assay (IFA) with 2-243a; anti-PDI, an ER marker; or MitoRed, which is a selective mitochondrial marker (Fig. 1G). TOM70 was associated with the mitochondria in all cells and was a part (~40%) of the ER, indicating that the TOM70 expressions in the mitochondria were higher than those in the ER.

TOM70 Inhibits TNF-α-Mediated Apoptotic Cell Death

The results of previous studies indicate the significant role of mitochondria in the apoptotic response [Hatano, 2007]. TOM70 interacts with Mcl-1 and facilitates mitochondrial targeting by the latter [Chou et al., 2006]. Mcl-1 silencing enhances TNF-related apoptosis-inducing ligand (TRAIL)-mediated cell death [Wirth et al., 2005; Han et al., 2006]. Therefore, the role of TOM70 in the apoptotic response was examined in this study. HepG2 cells were transfected with TOM70-pcDNA6 (Fig. 1D) or empty pcDNA6 (control), and their sensitivity to anti-Fas antibody (Fig. 2A) and TNF-α-mediated apoptotic cell death (Fig. 2B) was examined. When treated with 8 ng/ml of TNF-α, the TOM70-pcDNA6-transfected cells were significantly more viable than those transfected with empty pcDNA6 (Fig. 2B). In contrast, no significant differences were found between the viability of TOM70-pcDNA6 transfected cells and control cells treated with anti-Fas antibody (Fig. 2A). Thus, TNF-α-induced apoptosis was inhibited by TOM70 overexpression.

Interaction of TOM70 With HCV-NS3 and Other Host Factors

To determine the mechanism by which HCV induces TOM70, the TOM70 level in HCV NS3/4A-expressing HepG2 cells was determined (Fig. 3A). The TOM70 level was higher in the NS3/4A-expressing cells than in the control cells. Interestingly, the level of NS3/4A protein as well as Mcl-1 was reduced when TOM70 was silenced. The MAVS protein is cleaved by NS3/4A, as reported previously [Li et al., 2005], and the level of this protein was not influenced by the silencing of TOM70. IP-WB was performed to examine the possible interaction between TOM70 and NS3/4A (Fig. 3B). The pcDNA6-TOM70-myc plasmid was transfected into lenti-NS3/4A vector-transduced HepG2 cells; IP was performed using the anti-myc antibody, and the reaction was detected using the anti-NS3 antibody. The NS3 protein was

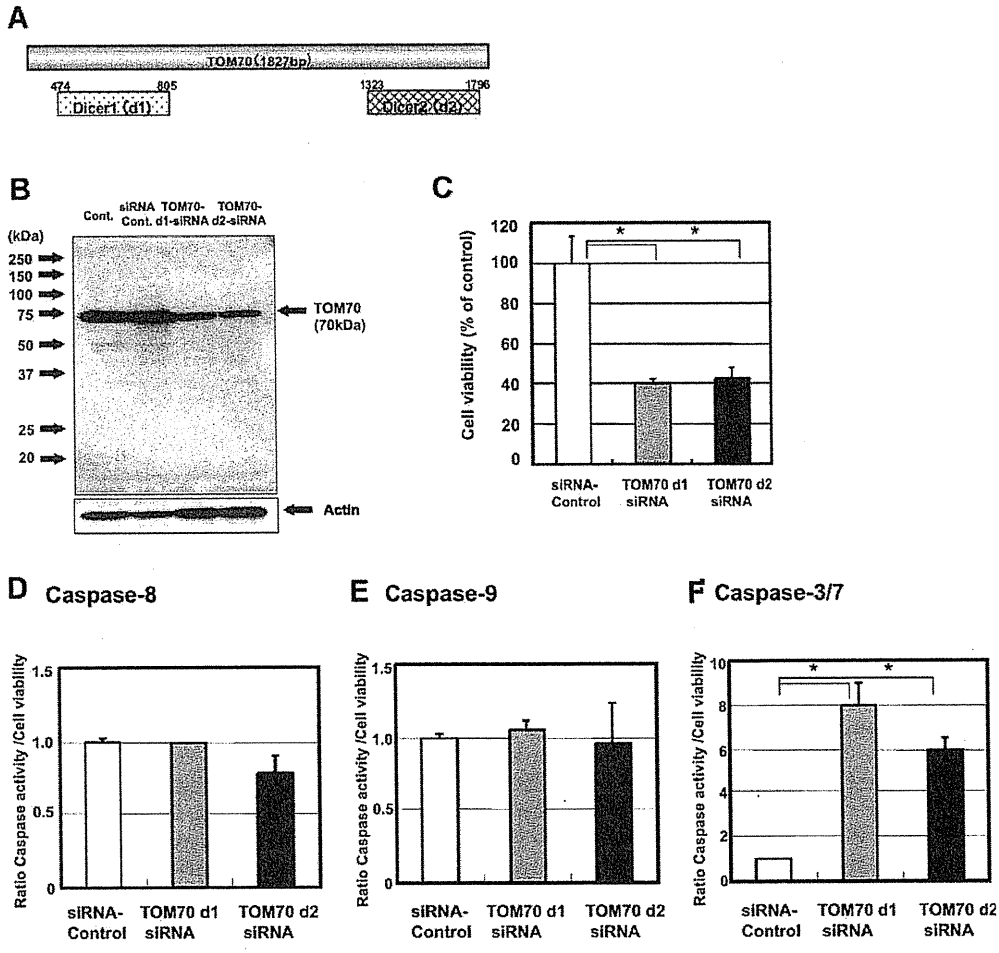

Fig. 4. Silencing of TOM70 induced apoptotic cell death and caspase-3/7 activity. **A**: The positions of TOM70-d1-siRNA and TOM70-d2-siRNA are indicated in the figure. **B**: siRNA-mediated silencing of TOM70 was detected by WB (Cont: no siRNA, siRNA Cont: siRNA control (Luci2-siRNA), TOM70-d1-siRNA, TOM70-d2-siRNA). **C**: TOM70 knockdown-induced cell death was calculated by measuring viability (%) with the WST-8 cell counting kit. The cell viability after 48 hr was scored in HepG2 cells transfected with the siRNA control Luci2-siRNA (□), TOM70-d1-siRNA (▩), and TOM70-d2-siRNA (■). The activities of caspase-8 (**D**), caspase-9 (**E**), and caspase-3/7 (**F**) were measured using commercially available assays and a luminometer. The caspase activity was scored after 48 hr in TOM70-knockdown HepG2 cells transfected with control siRNA (□), TOM70-d1-siRNA (▩), and TOM70-d2-siRNA (■). C–F: The data represent the average of the values obtained from triplicate experiments, and the vertical bars indicate the SD. $^{*}P < 0.05$ (two-tailed Student's *t*-test).

specifically precipitated by myc-tagged TOM70. The NS4A protein was not detected in this assay (data not shown). Therefore, the NS3 protein directly interacts with TOM70.

TOM70 Knockdown by RNAi Induces Apoptosis

The effect of TOM70 on the apoptotic response was examined because TOM70 silencing decreased the level of Mcl-1. First, two siRNAs for TOM70 (TOM70-d1-siRNA and TOM70-d2-siRNA) were designed in order to prevent the off-target effect (Fig. 4A). siRNA for luciferase (Luci-d2-siRNA) was used as a control (Fig. 4B). HepG2 cells were transfected with TOM70-d1-siRNA or TOM70-d2-siRNA, and the downregulation of TOM70 expression was confirmed by WB (Fig. 4B). Furthermore, decreased cell viability was observed (Fig. 4C) after 48 hr. Treatment with TOM70-d1-siRNA or TOM70-d2-siRNA significantly decreased the cell viability of HuH-7 cells too (data not shown). These results indicate that TOM70 silencing with siRNA may induce apoptosis.

The activities of caspase-3/7, caspase-8, and caspase-9 in HepG2 cells were examined after TOM70 silencing (Fig. 4D–F). The activities of caspase-8 and caspase-9 in cells transfected with TOM70 siRNA were not significantly different from those in the cells treated with control siRNA (Fig. 4D,E). In contrast, the caspase-3/7 activity in the TOM70-siRNA transfected cells was significantly greater than that in the cells treated with

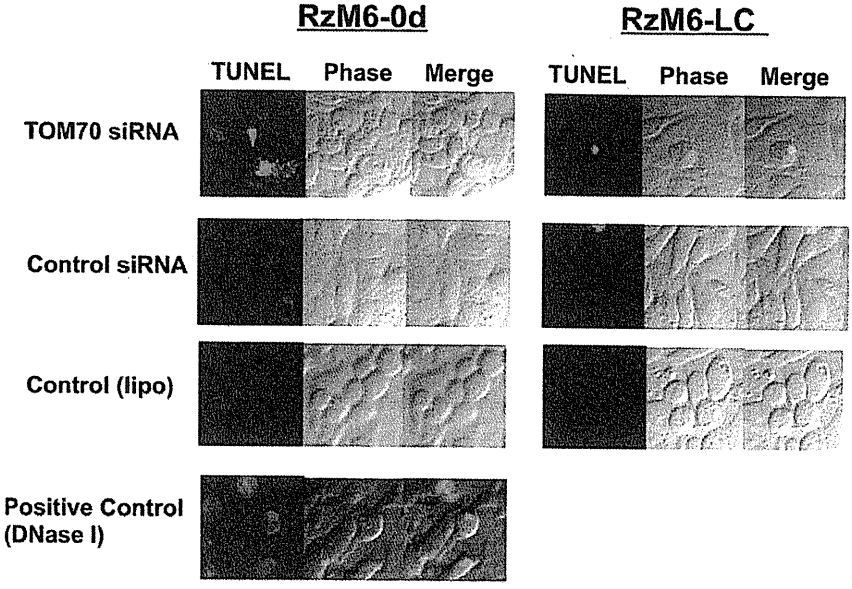

Fig. 5. TUNEL assay in RzM6-0d and RzM6-LC cells transfected with TOM70 siRNA, control siRNA, and control (Lipofectamine). The positive control is RzM6-0d cells treated with DNase I. The magnification is 400×.

control siRNA (Fig. 4F). These results indicate that the siRNA-mediated silencing of TOM70 expression induces apoptosis through caspase-3/7.

TOM70 Silencing-Induced Apoptosis Is Impaired by HCV

Next, the effect of TOM70 silencing-induced apoptosis was examined in RzM6-0d and RzM6-LC cells in order to determine the effect of HCV expression (Fig. 5). The apoptotic response was examined using the TUNEL assay wherein DNA strand breaks are detected and the apoptotic response is thereby detected [Gavrieli et al., 1992]. The DNA strand breaks, which were stained red, were observed using confocal microscopy. Treatment with TOM70 siRNA produced significant DNA strand breaks in the RzM6-0d cells. However, the apoptotic signal was suppressed in the RzM6-LC cells. This indicates the possibility that HCV can impair the apoptotic response induced by TOM70 siRNA.

Silencing of TOM70 Decreases Cell Viability, Whereas HCV-NS3 Restores Cell Viability

The RzM6-0d and RzM6-LC cells were treated with TOM70 siRNA and control siRNA, and the cell viability was measured using the WST-8 assay [Isobe et al., 1999] (Fig. 6A). The viability of the RzM6-LC cells was significantly higher than that of the RzM6-0d cells after treatment with TOM70 siRNA, and this difference increased in a dose-dependent manner. This indicates that the expression of HCV genes may impair the TOM70 siRNA-induced apoptotic response. The responsible HCV protein was identified using the lentivirus vector (Fig. 6B), and TOM70 siRNA-induced cell death was found to be impaired in HCV-NS3/4A-expressing cells.

DISCUSSION

The results of the present study suggest that HCV interacts with TOM70 through the NS3 protein, which indicates the possibility that TOM70 regulates the intracellular localization of HCV NS3; a previous study has reported the mitochondrion to be one of the regions where HCV NS3 is located [Sillanpaa et al., 2008]. The results of a previous study indicate that TOM70 also interacts with the Mcl-1 protein [Chou et al., 2006]. TOM70 silencing decreased the levels of the NS3 and Mcl-1 proteins; therefore, interaction with TOM70 may increase the stability of NS3 and Mcl-1. Recently, it was reported that Mcl-1 is stabilized by the deubiquitinase USP9X and that it can promote tumor cell survival [Schwickart et al., 2010]. Furthermore, Mcl-1 interacts with the HCV core protein through Bcl-2 homology domain 3 (BH3) [Mohd-Ismail et al., 2009], and Mcl-1 overexpression suppresses core-induced apoptosis. Therefore, further studies are required to clarify the relationship between TOM70, Mcl-1, and other host factors in HCV infection. This information may provide novel insights into the mechanism underlying the induction of apoptotic resistance and tumorigenicity in hepatocytes during chronic HCV infection.

The results of this study indicate the regulatory role of TOM70 in apoptosis. TOM70 overexpression was found to suppress the TNF-α-mediated but not the Fas-mediated apoptotic response. TOM70 knockdown

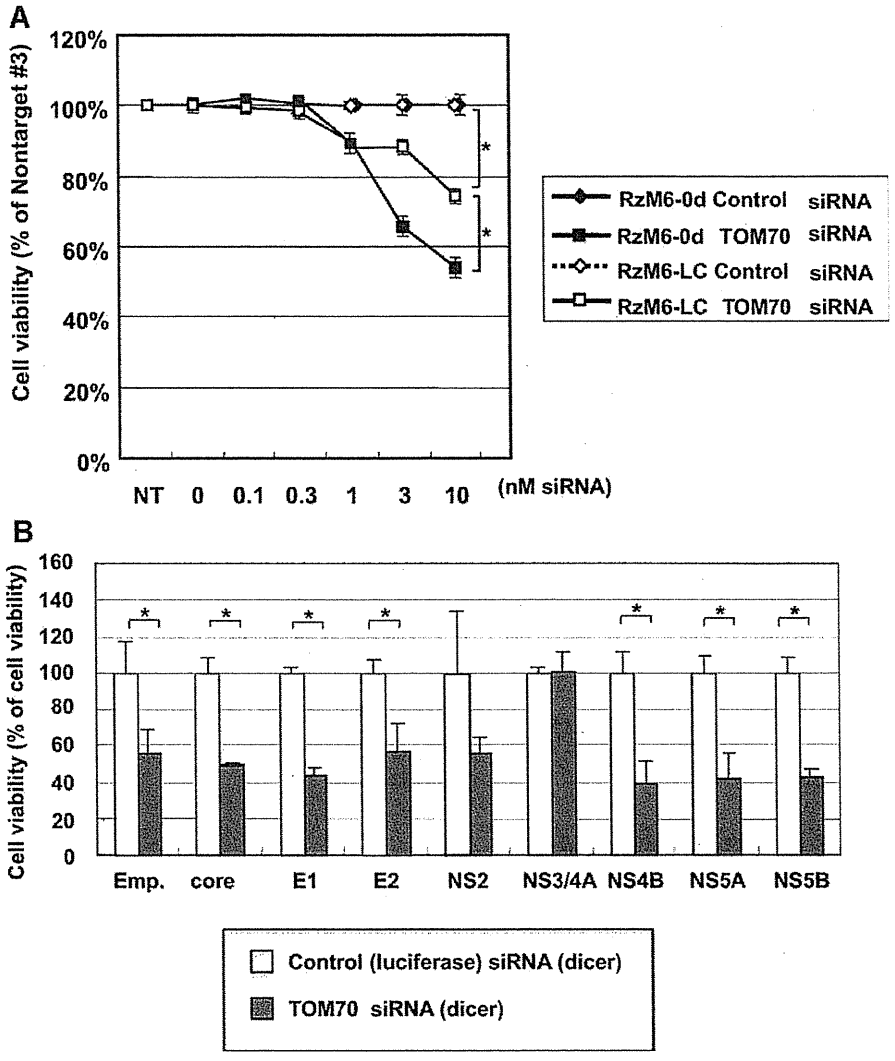

Fig. 6. **A:** Cell viability of RzM6-0d or RzM6-LC cells after treatment with TOM70 siRNA. The viability is given as the ratio (%) of test to control siRNA treatment. **B:** The viability of HepG2 cells transduced with lentivirus vectors expressing the HCV core, E1, E2, NS2, NS3/4A, NS4B, NS5A, and NS5B proteins after treatment with TOM70 siRNA was measured by the WST assay, and the viability is given as the ratio (%) of the test to the control siRNA treatment. The data represents the average of the values obtained from triplicate experiments, and the vertical bars indicate SD. $^*P < 0.05$ (two-tailed Student's *t*-test).

increased caspase-3/7 activity, but the activities of caspase-8 and caspase-9 were not significantly affected. This indicates the possibility that TOM70 regulates the TNF receptor-mediated apoptotic pathway. Several reports have indicated that TNF-α-mediated apoptosis is inhibited by HCV proteins. Saito et al. [2006] reported that the HCV core protein inhibited the TNF-α-mediated signaling pathway through the sustained expression of a cellular- FADD-like interleukin-1β-converting enzyme (FLICE) like inhibitory protein (c-FLIP; caspase-8 inhibitor). Majumder et al. [2002] reported that TNF-α-mediated hepatic apoptosis was impaired by the HCV-NS5A protein. The results of the present study revealed an alternative pathway by which HCV can acquire TNF-α-induced apoptotic resistance through TOM70 augmentation. Recently, it has been reported that TOM70 interacts with MAVS, TNFRSF1A-associated via death domain (TRADD), TNF receptor-associated factor 6 (TRAF6), stimulator of interferon genes (STING), and interferon regulatory factor (IRF)-3, and that augmentation of TOM70 activates retinoic acid-inducible gene (RIG)-I signaling [Liu et al., 2010]. The results of recent studies indicate that IRF-3 can activate Bax expression and apoptosis [Chattopadhyay et al., 2004]. Future studies on the modification of the regulatory pathway of TOM70 by HCV may provide further insights on the mechanism underlying persistent HCV infection.

ACKNOWLEDGMENTS

The authors thank Dr. H. Fukuda and Dr. S. Ohmi for their technical support with regard to MALDI-TOF-MS analysis, Dr. F. Yasui and Dr. T. Munakata for their critical comments, Dr. Satoh for his technical support, and Prof. S. Harada for his support.

REFERENCES

Chattopadhyay S, Marques JT, Yamashita M, Peters KL, Smith K, Desai A, Williams BR, Sen GC. 2004. Viral apoptosis is induced by IRF-3-mediated activation of Bax. EMBO J 29:1762–1773.

Chou CH, Lee RS, Yang-Yen HF. 2006. An internal EELD domain facilitates mitochondrial targeting of Mcl-1 via a Tom70-dependent pathway. Mol Biol Cell 17:3952–3963.

Deng L, Adachi T, Kitayama K, Bungyoku Y, Kitazawa S, Ishido S, Shoji I, Hotta H. 2008. Hepatitis C virus infection induces apoptosis through a Bax-triggered, mitochondrion-mediated, caspase 3-dependent pathway. J Virol 82:10375–10385.

Gavrieli Y, Sherman Y, Ben-Sasson SA. 1992. Identification of programmed cell death in situ via specific labeling of nuclear DNA fragmentation. J Cell Biol 119:493–501.

Han J, Goldstein LA, Gastman BR, Rabinowich H. 2006. Interrelated roles for Mcl-1 and BIM in regulation of TRAIL-mediated mitochondrial apoptosis. J Biol Chem 281:10153–10163.

Hatano E. 2007. Tumor necrosis factor signaling in hepatocyte apoptosis. J Gastroenterol Hepatol 22:S43–S44.

Hoogenraad NJ, Ward LA, Ryan MT. 2002. Import and assembly of proteins into mitochondria of mammalian cells. Biochim Biophys Acta 1592:97–105.

Isobe I, Michikawa M, Yanagisawa K. 1999. Enhancement of MTT, a tetrazolium salt, exocytosis by amyloid beta-protein and chloroquine in cultured rat astrocytes. Neurosci Lett 266:129–132.

Jensen ON, Wilm M, Shevchenko A, Mann M. 1999. Sample preparation methods for mass spectrometric peptide mapping directly from 2-DE gels. Methods Mol Biol 112:513–530.

Lei Y, Moore CB, Liesman RM, O'Connor BP, Bergstralh DT, Chen ZJ, Pickles RJ, Ting JP. 2009. MAVS-mediated apoptosis and its inhibition by viral proteins. PLoS One 4:e5466.

Li XD, Sun L, Seth RB, Pineda G, Chen ZJ. 2005. Hepatitis C virus protease NS3/4A cleaves mitochondrial antiviral signaling protein off the mitochondria to evade innate immunity. Proc Natl Acad Sci USA 102:17717–17722.

Liu XY, Wei B, Shi HX, Shan YF, Wang C. 2010. Tom70 mediates activation of interferon regulatory factor 3 on mitochondria. Cell Res 20:994–1011.

Majumder M, Ghosh AK, Steele R, Zhou XY, Phillips NJ, Ray R, Ray RB. 2002. Hepatitis C virus NS5A protein impairs TNF-mediated hepatic apoptosis, but not by an anti-FAS antibody, in transgenic mice. Virology 294:94–105.

Mihara K, Omura T. 1996. Cytoplasmic chaperones in precursor targeting to mitochondria: The role of MSF and hsp 70. Trends Cell Biol 6:104–108.

Mohd-Ismail NK, Deng L, Sukumaran SK, Yu VC, Hotta H, Tan YJ. 2009. The hepatitis C virus core protein contains a BH3 domain that regulates apoptosis through specific interaction with human Mcl-1. J Virol 83:9993–10006.

Neupert W. 1997. Protein import into mitochondria. Annu Rev Biochem 66:863–917.

Nishimura T, Kohara M, Izumi K, Kasama Y, Hirata Y, Huang Y, Shuda M, Mukaidani C, Takano T, Tokunaga Y, Nuriya H, Satoh M, Saito M, Kai C, Tsukiyama-Kohara K. 2009. Hepatitis C virus impairs p53 via persistent overexpression of 3beta-hydroxysterol Delta24-reductase. J Biol Chem 284:36442–36452.

Nomura-Takigawa Y, Nagano-Fujii M, Deng L, Kitazawa S, Ishido S, Sada K, Hotta H. 2006. Non-structural protein 4A of Hepatitis C virus accumulates on mitochondria and renders the cells prone to undergoing mitochondria-mediated apoptosis. J Gen Virol 87: 1935–1945.

Pfanner N, Geissler A. 2001. Versatility of the mitochondrial protein import machinery. Nat Rev Mol Cell Biol 2:339–349.

Pfanner N, Meijer M. 1997. The Tom and Tim machine. Curr Biol 7:R100–R103.

Saito K, Meyer K, Warner R, Basu A, Ray RB, Ray R. 2006. Hepatitis C virus core protein inhibits tumor necrosis factor alpha-mediated apoptosis by a protective effect involving cellular FLICE inhibitory protein. J Virol 80:4372–4379.

Saitou K, Mizumoto K, Nishimura T, Kai C, Tsukiyama-Kohara K. 2009. Hepatitis C virus-core protein facilitates the degradation of Ku70 and reduces DNA-PK activity in hepatocytes. Virus Res 144: 266–271.

Schatz G. 1996. The protein import system of mitochondria. J Biol Chem 271:31763–31766.

Schwickart M, Huang X, Lill JR, Liu J, Ferrando R, French DM, Maecker H, O'Rourke K, Bazan F, Eastham-Anderson J, Yue P, Dornan D, Huang DC, Dixit VM. 2010. Deubiquitinase USP9X stabilizes MCL1 and promotes tumour cell survival. Nature 463: 103–107.

Seeff LB. 2002. Natural history of chronic hepatitis C. Hepatology 36:S35–S46.

Sillanpaa M, Kaukinen P, Melen K, Julkunen I. 2008. Hepatitis C virus proteins interfere with the activation of chemokine gene promoters and downregulate chemokine gene expression. J Gen Virol 89:432–443.

Stojanovski D, Johnston AJ, Streimann I, Hoogenraad NJ, Ryan MT. 2003. Import of nuclear-encoded proteins into mitochondria. Exp Physiol 88:57–64.

Truscott KN, Pfanner N, Voos W. 2001. Transport of proteins into mitochondria. Rev Physiol Biochem Pharmacol 143:81–136.

Tsukiyama-Kohara K, Tone S, Maruyama I, Inoue K, Katsume A, Nuriya H, Ohmori H, Ohkawa J, Taira K, Hoshikawa Y, Shibasaki F, Reth M, Minatogawa Y, Kohara M. 2004. Activation of the CKI-CDK-Rb-E2F pathway in full genome hepatitis C virus-expressing cells. J Biol Chem 279:14531–14541.

Wakita T, Pietschmann T, Kato T, Date T, Miyamoto M, Zhao Z, Murthy K, Habermann A, Krausslich HG, Mizokami M, Bartenschlager R, Liang TJ. 2005. Production of infectious hepatitis C virus in tissue culture from a cloned viral genome. Nat Med 11: 791–796.

Wirth T, Kuhnel F, Fleischmann-Mundt B, Woller N, Djojosubroto M, Rudolph KL, Manns M, Zender L, Kubicka S. 2005. Telomerase-dependent virotherapy overcomes resistance of hepatocellular carcinomas against chemotherapy and tumor necrosis factor-related apoptosis-inducing ligand by elimination of Mcl-1. Cancer Res 65:7393–7402.

Research Article

EASL EUROPEAN ASSOCIATION FOR THE STUDY OF THE LIVER | JOURNAL OF HEPATOLOGY

Augmentation of DHCR24 expression by hepatitis C virus infection facilitates viral replication in hepatocytes

Takashi Takano[1,†], Kyoko Tsukiyama-Kohara[2,*], Masahiro Hayashi[1], Yuichi Hirata[1], Masaaki Satoh[2], Yuko Tokunaga[1], Chise Tateno[3], Yukiko Hayashi[4], Tsunekazu Hishima[4], Nobuaki Funata[4], Masayuki Sudoh[5], Michinori Kohara[1]

[1]*Department of Microbiology and Cell Biology, Tokyo Metropolitan Institute of Medical Science, 2-1-6 Kamikitazawa, Setagaya-ku, Tokyo 156-8506, Japan;* [2]*Department of Experimental Phylaxiology, Faculty of Medical and Pharmaceutical Sciences, Kumamoto University, 1-1-1 Honjo, Kumamoto, Kumamoto 860-8556, Japan;* [3]*Phoenix Bio Co., Ltd., Study Service Department, 3-4-1 Kagamiyama, Higashi-Hiroshima 739-0046, Japan;* [4]*Department of Pathology, Tokyo Metropolitan Komagome Hospital, 3-18-22 Honkomagome, Bunkyo-ku, Tokyo 113-8677, Japan;* [5]*Kamakura Research Laboratories, Chugai Pharmaceutical Co., Ltd., Kajiwara 200, Kamakura-City, Kanagawa 247-8530, Japan*

Background & Aims: We characterized the role of 24-dehydrocholesterol reductase (DHCR24) in hepatitis C virus infection (HCV). DHCR24 is a cholesterol biosynthetic enzyme and cholesterol is a major component of lipid rafts, which is reported to play an important role in HCV replication. Therefore, we examined the potential of DHCR24 as a target for novel HCV therapeutic agents.

Methods: We examined DHCR24 expression in human hepatocytes in both the livers of HCV-infected patients and those of chimeric mice with human hepatocytes. We targeted *DHCR24* with siRNA and U18666A which is an inhibitor of both DHCR24 and cholesterol synthesis. We measured the level of HCV replication in these HCV replicon cell lines and HCV infected cells. U18666A was administrated into chimeric mice with humanized liver, and anti-viral effects were assessed.

Results: Expression of DHCR24 was induced by HCV infection in human hepatocytes *in vitro*, and in human hepatocytes of chimeric mouse liver. Silencing of *DHCR24* by siRNA decreased HCV replication in replicon cell lines and HCV JFH-1 strain-infected cells. Treatment with U18666A suppressed HCV replication in the replicon cell lines. Moreover, to evaluate the anti-viral effect of U18666A *in vivo*, we administrated U18666A with or without pegylated interferon to chimeric mice and observed an inhibitory effect of U18666A on HCV infection and a synergistic effect with interferon.

Conclusions: DHCR24 is an essential host factor which augmented its expression by HCV infection, and plays a significant role in HCV replication. DHCR24 may serve as a novel anti-HCV drug target.

Introduction

Extensive epidemiological studies have identified multiple risk factors for hepatocellular carcinoma (HCC), including chronic infection with hepatitis C virus (HCV), and hepatitis B virus (HBV), and cirrhosis due to non-viral etiologies, such as alcohol abuse and aflatoxin B1 exposure [1,2]. Of these factors, HCV appears to be the dominant causative factor for HCC in many developed countries. The World Health Organization estimates that 170 million people worldwide are infected with HCV and are, therefore, at risk of developing liver cirrhosis and HCC [3]. The combination of pegylated interferon-α (PEG-IFN-α) and ribavirin is currently the standard treatment regimen for patients with chronic HCV infection. However, viral clearance is achieved in only 40% to 60% of patients and depends on the HCV genotype with which the patient is infected [4].

We previously established the RzM6 cell line, a HepG2 cell line in which the full-length HCV genome (HCR6-Rz) can be conditionally expressed under control of the Cre/*lox*P system and is precisely self-trimmed at the 5′ and 3′-termini by ribozyme sequences [5]. Anchorage-independent growth of these cells accelerates after 44 days of continuous passaging, during which the Cdk-Rb-E2F pathway is activated [5]. In a previous study, we developed monoclonal antibodies (MoAbs) against cell surface antigens on HCV-expressing cells that had been passaged for over 44 days [6]. One of the targets of these MoAbs was 24-dehydrocholesterol reductase (DHCR24 is also called 3-β-hydroxysterol-Δ-24-reductase, seladin-1, desmosterol delta-24-reductase), a molecule that is frequently overexpressed in the hepatocytes of HCV-infected patients.

Keywords: Hepatitis C virus; Replication; DHCR24; U18666A.
Received 18 April 2010; received in revised form 11 November 2010; accepted 2 December 2010; available online 22 December 2010

* Corresponding author. Address: Department of Experimental Phylaxiology, Faculty of Life Sciences, Kumamoto University, 1-1-1 Honjo, Kumamoto, Kumamoto 860-8556, Japan. Tel./fax: +81 96 373 5560.
E-mail address: kkohara@kumamoto-u.ac.jp (K. Tsukiyama-Kohara).
† Present address: Division of Veterinary Public Health, Nippon Veterinary and Life Science University, 1-7-1 Kyonan, Musashino, Tokyo 180-8602, Japan.

Abbreviations: DHCR24, 24-dehydrocholesterol reductase; HCV, hepatitis C virus; MoAb, monoclonal antibody; HCC, hepatocellular carcinoma; HBV, hepatitis B virus.

ELSEVIER

Journal of Hepatology **2011** vol. 55 | 512–521

DHCR24 confers resistance to apoptosis in neuronal cells [7]. It also regulates the cellular response to oxidative stress by binding to the amino terminus of p53, thereby displacing mouse double minute 2 homolog isoform MDM2 (*Homo sapiens*) (MDM2) from p53 and inducing the accumulation of p53 in human embryonic fibroblasts [8].

DHCR24 is a cholesterol biosynthetic enzyme that is also called desmosterol reductase [9,10]. Cholesterol is a major component of lipid rafts, which are reported to play an important role in HCV replication [11]. Therefore, we characterized the role of DHCR24 in HCV replication and evaluated its potential as a target for novel HCV therapeutic agents. We also examined the synergistic antiviral effect of U18666A which is an inhibitor of both DHCR24 [12] and cholesterol synthesis [13] with IFN-α in the treatment of HCV.

Materials and methods

Cells and plasmids

Cell culture methods of the HuH-7 [14], HepG2 [15], hybridoma and myeloma PAI cells, RzM6 cells [5], and the HCV subgenomic replicon cells lines FLR3-1 (genotype 1b, strain Con-1; [16]), R6FLR-N (genotype 1b, strain N; [17]), and Rep JFH Luc3-13) genotype 2a, strain JFH-1 [18]) were utilized to evaluate HCV replication [19] are described in Supplementary data.

The *DHCR24* cDNA was synthesized and amplified by PCR using Phusion™ DNA polymerase (Finnzymes) and cloned into the pcDNA3.1 vector (Invitrogen) or lentivirus vector, as described previously [6].

Matrix-assisted laser desorption ionization time-of-flight mass spectrometry analysis

The detailed procedures are described in Supplementary data [20].

Immunohistochemistry and Western blot analysis

The detailed procedures are described in Supplementary data.

The antibodies used in this experiment were: anti-Core, anti-NS3, anti-NS4B, anti-NS5B [5], and anti-NS5A (kindly provided by Dr. Matsuura, Osaka University), and anti-actin (Sigma).

Inhibition of DHCR24 by siRNA

We synthesized two siRNAs that were directed against human *DHCR24* mRNA: siDHCR24-417 and siDHCR24-1024. The target sequence of siDHCR24-417 was 5'-GUACAAGAAGACACACAAATT-3', while that of siDHCR24-1024 was 5'-GAGAACUAUCUGAAGACAATT-3'. Additionally, we used siRNAs targeted against the HCV genome (siE-R7 and siE-R5) [17,21]. The siCONTROL Non-Targeting siRNA #3 (Dharmacon RNA Technologies) was used as the negative control siRNA. The chemically synthesized siRNAs were transfected into cells using Lipofectamine RNAiMAX (Invitrogen) and Opti-MEM (Invitrogen) by reverse-transfection. Cells were characterized 72 h after transfection.

Inhibition of viral replication by U18666A

U18666A (Calbiochem) was utilized to treat HCV replicon cells at a concentration of 62.5–1000 nM and chimeric mice at a concentration of 10 mg/kg (i.p.).

To determine whether cholesterol can reverse the U18666A treatment by the addition of cholesterol, we performed the experiments using HCV replicon cells (4×10^3 cells/well in a 96-well white plate, SUMILON). Culture medium was replaced after the cells had spread (at 24 h), and LDL (Calbiochem) was added to reach a final cholesterol concentration of 50 μg/ml. After a 24 h-incubation, U18666A (62.5, 125, 250, 500, and 1000 nM) was added to each well, and the cells were incubated for an additional 48 h. HCV replication activity was measured by luciferase assay, and cell viability was measured with the WST-8 cell counting kit according to the manufacturer's instructions (Dojindo Laboratories). Cholesterol measurements are described in Supplementary data.

Inhibition assay of HCV replication in replicon cells and persistent infected cells

For evaluation of the anti-HCV replication effect of the inhibitor U18666A in replicon cells and HCV persistently infected cells are described in Supplementary data.

Real-time detection (RTD)-PCR

Total RNA was purified from JFH-K4 cells that had been treated with siRNA or U18666A by the acid guanidium–phenol–chloroform method. HCV RNA was quantified by RTD-PCR as previously described [22].

HCV infection of chimeric mice with humanized liver and mRNA quantification by RTD-PCR

We used chimeric mice that were created by transplanting human primary hepatocytes into severe combined immunodeficient mice carrying a urokinase plasminogen activator transgene [23,24] that was controlled by the albumin promoter. These hepatocytes had been infected with plasma from a HCV-positive patient HCR6 (genotype 1b) [19]. The HCV 1b RNA level reached 2.9–18.0 × 10^6 copies/ml in mouse sera after 1–2 months of infection. HCV RNA in the mouse serum or total RNA from liver tissue from humanized chimeric mice with/without HCV infection was extracted using the acid guanidium–phenol–chloroform method. HCV RNA and *DHCR24* mRNA levels were quantified by RTD-PCR [22]. The primers and probes for HCV were prepared as previously described [22], and the primers and probes for *DHCR24* were prepared using TaqMan® Gene Expression assays (Applied Biosystems) according to the manufacturer's instructions. PEG-IFNα-2a (Chugai) was administered subcutaneously at a concentration of 30 μg/kg, at day 1, 4, 8, and 11 (the amount of PEG-IFN-α administered to the chimeric mice was 20-fold relative to that used in humans), and U18666A was administered intraperitoneally at a concentration of 10 mg/kg, every day for 2 weeks (Fig. 6A). The protocols for the animal experiments were approved by the local ethics committee.

Human serum albumin in the blood of humanized chimeric mice was measured using a commercially available kit, according to the manufacturer's instructions (Alb-II kit; Eiken Chemical).

Results

Identification of DHCR24

We inoculated mice (BALB/c) with RzM6 cells that expressed HCV protein and had been cultured for over 44 days (denoted as RzM6-LC cells); mice were inoculated at least seven times over a 2-week period. We then fused the splenocytes from mice that had been immunized with RzM6-LC cells to myeloma cells to establish hybridomas. Characterization of the culture supernatant from more than 1000 hybridoma cells by ELISA (data not shown) revealed that one MoAb clone (2-152a) recognized a molecule of approximately 60 kDa in various cells (Supplementary Fig. 1A and B. This molecule was more highly expressed in RzM6-LC cells (Supplementary Fig. 1A), HeLa cells, and HCC cell lines (HepG2, HuH-7, Hep3B, and PLC/PRF/5) than in HEK293 cells and several normal liver cell lines (NKNT, TTNT, and WRL68) (Supplementary Fig. 1B). To further characterize this molecule, we performed matrix-assisted laser desorption ionization time-of-flight mass spectrometry (MALDI-TOF-MS) and obtained seven peptide sequences (Supplementary Fig. 1C, underlined). These peptide sequences suggested that the molecule that was recognized by the 2-152a antibody was DHCR24. We constructed a lentivirus expression vector containing myc-tagged DHCR24 (DHCR24-myc) and transduced it into HepG2 cells. By western blot analysis with 2-152a and anti-Myc antibody, we then confirmed that DHCR24 was expressed in the transduced cells (Supplementary Fig. 1D). We found that the 2-152a antibody specifically recognized DHCR24.

Research Article

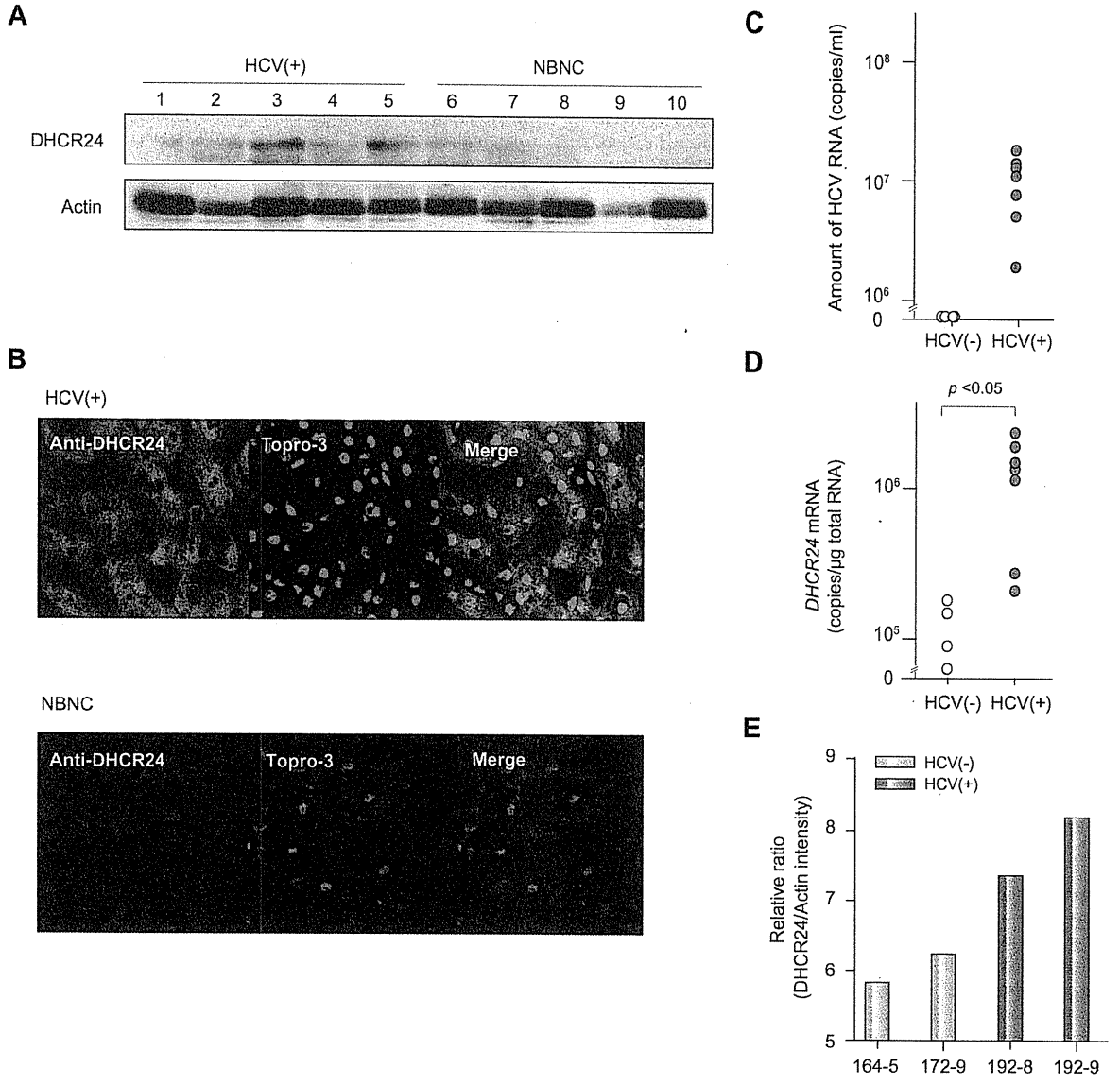

Fig. 1. HCV induces DHCR24 overexpression *in vitro* and *in vivo*. (A) Expression of DHCR24 in non-cancerous regions of livers of HCV-infected (+) and NBNC-HCC patients. Lysates (25 μg/lane) of non-cancerous liver tissues from HCC patients were analyzed by Western blot analysis using MoAb 2-152a. The patient numbers (Supplementary Table 1) are indicated at the top of the blot. (B) Immunohistochemical staining of HCV-infected non-cancerous tissues derived from an HCC patient using the monoclonal antibody 2-152a (Alexa488), anti-TO-PRO-3, or a merge (600× magnification) (upper panel). Tissues from an NBNC patient stained with the monoclonal antibody 2-152a (Alexa488) as well as TO-PRO-3 (640× magnification) (lower panel). (C) The amount of HCV RNA that was present in the HCV-R6 (genotype 1b)-infected chimeric mice with the humanized liver was quantified using RTD-PCR. The results of HCV uninfected ($n = 4$) and infected ($n = 7$) is indicated. (D) The amount of *DHCR24* mRNA present in total RNA isolates of HCV-R6 (genotype 1b)-infected chimeric mice with the humanized liver was quantified using RTD-PCR. *$p < 0.05$ (Mann–Whitney test). The results of HCV uninfected ($n = 4$) and infected ($n = 7$) are indicated. (E) DHCR24 protein was detected by Western blot analysis using MoAb 2-152a as a probe, and quantitated by LAS3000. Protein levels are normalized to actin and ratio is indicated.

HCV infection in vivo induces persistent overexpression of DHCR24

We next examined whether HCV infection could induce DHCR24 expression in human hepatocytes. DHCR24 was overexpressed more frequently in liver tissues from HCV-positive patients than in tissues from HBV- and HCV-negative (NBNC) patients (Fig. 1A and Supplementary Table 1). The liver tissue from HCV-positive patients stained more strongly for DHCR24 expression than the liver tissue from NBNC patients (Fig. 1B). We inoculated chimeric mice [19,23,25] with HCV ($10^{6.2}$ copies/ml) that had been isolated from the plasma of HCV-infected patients (patient R6, HCV genotype 1b). The serum concentration of human albumin (Supplementary Fig. 2A) in the chimeric mice after transplantation of hepatocytes indicated that human hepatocytes had engrafted in the mouse livers. Thirty days after transplantation, mice were infected with HCV, and HCV and RNA titers were analyzed both

before and after inoculation (Supplementary Fig. 2B). The average amount of HCV RNA that was present in the serum of the infected chimeric mice at 28 days post-infection was 1.1×10^7 copies/ml (Fig. 1C and Supplementary Fig. 2B). The *DHCR24* mRNA levels in the livers of the chimeric mice were also quantified at 28 days post-infection by real-time detection (RTD)-PCR [22]. The results revealed that there was a significant increase in *DHCR24* expression as measured by mRNA levels in HCV infected chimeric mice (Fig. 1D). Next, we examined the extent to which translation of DHCR24 occurred in the chimeric mice (Fig. 1E), higher DHCR24 protein levels were present in hepatocytes from HCV-infected mice (Nos. 192-8 and 192-9) than in those of uninfected mice (Nos. 164-5 and 172-9). These findings indicate that expression of DHCR24 is significantly up-regulated by HCV infection in human hepatocytes.

Role of DHCR24 in HCV replication

Since augmentation of DHCR24 expression was observed by HCV infection in humanized chimeric mice, we next examined whether DHCR24 was involved in HCV replication or not. We transfected siRNA into HCV replicon cell lines FLR3-1 (Fig. 2A and B) and R6FLR-N (Fig. 2C and D). Treatment with either two different *DHCR24* siRNA molecules (siDHCR24-417 or -1024) decreased HCV replication in a dose-dependent manner (Fig. 2A and C) but did not appear to have a significant effect on cell viability (Fig. 2B and D). Western blot analysis using HCV subgenomic replicon cell lines confirmed these findings (Fig. 2E and F). We also transfected the *DHCR24* siRNAs into HCV JFH-1 strain [18]-infected HuH7/K4 cell lines and found, by Western blot analysis, that the siRNAs inhibited HCV protein expression (Fig. 2G and H). These results indicate that DHCR24 may play a role in HCV replication.

The expression level of DHCR24 is linked to intracellular cholesterol levels

Human DHCR24 is involved in cholesterol biosynthesis [10]. It participates in multiple steps of cholesterol synthesis from lanosterol [26] (Fig. 3A). To examine the effect of cholesterol on the DHCR24 expression level in HuH-7 cells, we added cholesterol to cultured cells and determined the DHCR24 expression level (Fig. 3B). Expression levels of DHCR24 in HuH-7 cells were decreased approximately 50% by addition of cholesterol compared to that of the untreated control (Fig. 3B). On the other hand, that of DHCR24 in HepG2 cells was increased 2.5-fold by depletion of cholesterol using methyl-β-cyclodextrin (M-β-CD) (Fig. 3C).

These results indicate that the expression of DHCR24 in a cell correlates with the cholesterol level in that cell. Furthermore, silencing *DHCR24* reduced the cholesterol level in cells compared to control cells (Fig. 3D), suggesting that DHCR24 is essential for cholesterol synthesis.

Effect of U18666A on HCV replication in vitro

We further examined the role that DHCR24 plays in HCV replication by treating cells with U18666A. Treatment with U18666A (62.5, 125, 250, 500, and 1000 nM) of HCV replicon cells (FLR3-1) decreased HCV replication in a dose-dependent manner as shown by luciferase assay (Fig. 4A) and Western blot analysis (Fig. 4B). Notably, DHCR24 protein appeared as doublet bands in the absence of U18666A, but the lower band shifted to the upper band after treatment with U18666A (Fig. 4B). U18666A also suppressed HCV replication in other replicon cell lines (R6FLR-N and Rep JFH Luc 3-13; Fig. 4C and D). Treatment with U18666A (<250 nM) suppressed viral replication without producing significant cytotoxicity. We also examined the effect of 7-dehydrocholesterol reductase (DHCR7) (Fig. 3A) on HCV replication using the specific inhibitor BD1008 [26]. Treatment with BD1008 also suppressed HCV replication, but the concentration required was much higher than that needed in the U18666A assays (Fig. 4E); the concentration also greatly exceeded the intrinsic IC_{50} value for inhibition of σ-receptor binding (47 ± 2 nM) [27]. Therefore, DHCR24 may play a more significant role than DHCR7 in HCV replication. We next evaluated the compensatory effect that the addition of cholesterol had on cells treated with U18666A (Fig. 4F and G) by examining low density lipoprotein (LDL)-replaceable dissolved cholesterol levels as described in Supplementary data. Treatment with cholesterol led to partial restoration of HCV replication (Fig. 4F). These results suggest that U18666A suppresses HCV replication by depleting cellular cholesterol stores.

Next, we characterized the effect that U18666A had on HCV JFH-1 infection. Adding U18666A (62.5, 125, 250, and 500 nM) to HCV JFH-1-infected cell lines for 72 h, reductions of NS5B protein level were observed in cells treated more than 500 nM of U18666A (Fig. 5A and B). Additionally, the HCV RNA copy number in infected cells was suppressed by addition of 250 or 500 nM of U18666A (Fig. 5C). Examination of the cytotoxicity that U18666A (62.5–500 nM) had on infected cells revealed that it had little effect on cell viability (Fig. 5D). These results demonstrate that inhibition of DHCR24 by U18666A suppresses viral replication in HCV replicon cells and HCV-infected cells.

Evaluation of the anti-HCV effect of U18666A in vivo

To examine the effect of U18666A on HCV infection *in vivo*, we administered U18666A to HCV-infected chimeric mice with the humanized liver. The mice were infected with HCV via inoculation of patient serum HCR6 5 weeks after transplantation of human hepatocytes. U18666A (10 mg/kg) and PEG-IFN-α (30 μg/kg) were then administrated to these mice for 2 weeks (Fig. 6A). HCV RNA quantity (Fig. 6B) and serum human albumin levels (Fig. 6C) were measured in the mice after 1, 4, and 14 days of HCV infection. Treatment with U18666A alone significantly decreased HCV RNA levels in the serum (from 1×10^8 to 3×10^5 copies/ml) after 2 weeks, and its suppressive effect was more pronounced than that of PEG-IFN-α alone (8×10^5 copies/ml; Fig. 6B). Moreover, co-administration of U18666A and PEG-IFN-α synergistically (combination index <1) enhanced the antiviral effect of PEG-IFN-α (5×10^4 copies/ml). Treatment with these drugs did not significantly affect the serum human albumin concentrations in treated mice (Fig. 6C).

Discussion

The results of this study revealed that DHCR24, an enzyme that participates in cholesterol synthesis (last step; Fig. 3A), also plays a significant role in HCV replication. To our knowledge, this is the first report that this molecule is involved in HCV infection. The mevalonate route of the cholesterol synthesis pathway (starting from acetyl Co-A) has previously been reported to be involved in

Research Article

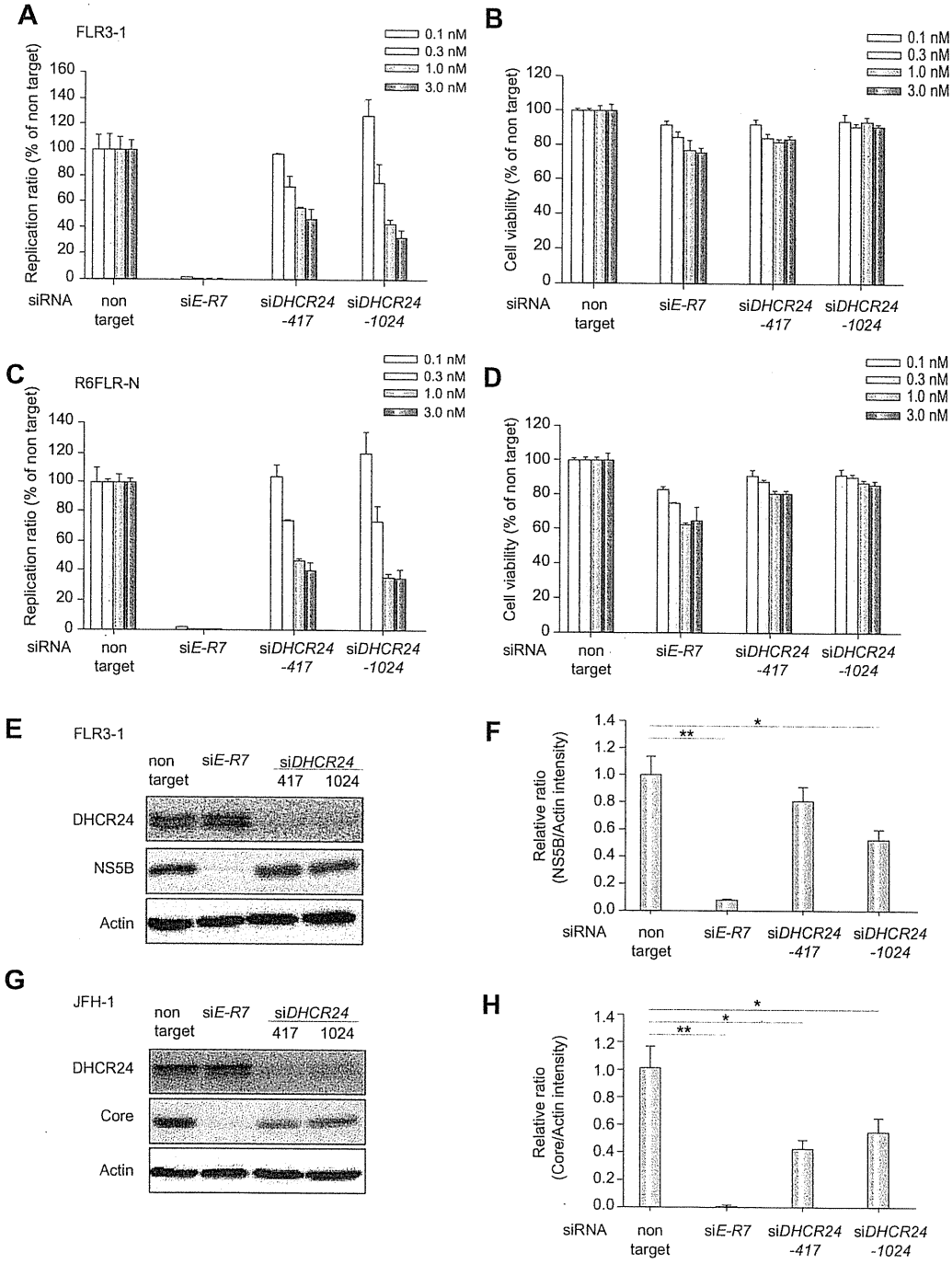

Fig. 2. Effect of DHCR24 knockdown on HCV replication. (A–D) Effect of DHCR24 knockdown on HCV replication in HCV replicon cells (FLR3-1 and R6FLR-N) at 72 h after the anti-*DHCR24* siRNAs (417 and 1024), siRNAs against HCV (siE-R7 for FLR3-1 and JFH-1; siE-R5 for R6-FLR-N), or non-target control siRNAs were transfected into HCV replicon cells. Replication activity was examined by luciferase assay (A and C), and cell viability was measured by the WST-8 assay (B and D). The data represent the mean of three experiments, and the bars indicate SD values. The Western blot analysis (E) and relative intensity of HCV-NS5B protein band was measured by LAS3000 and normalized with that of actin (F) after the treatment with siRNAs targeted against *DHCR24* (siDHCR24-417 and 1024) or HCV (si*E-R7*) in FLR3-1 replicon cells. (G and H) In HCV JFH-1-infected cells, DHCR24 knockdown by si*DHCR*24-417 and 1024 and HCV knockdown by siE-R7 were performed, and DHCR24 and HCV core protein expressions were confirmed by Western blot analysis. The relative intensity ratio of core protein to actin is indicated (H). The data represent the mean of three experiments, and the bars indicate SD values. *p <0.05, **p <0.01 (two-tailed Student's t test).

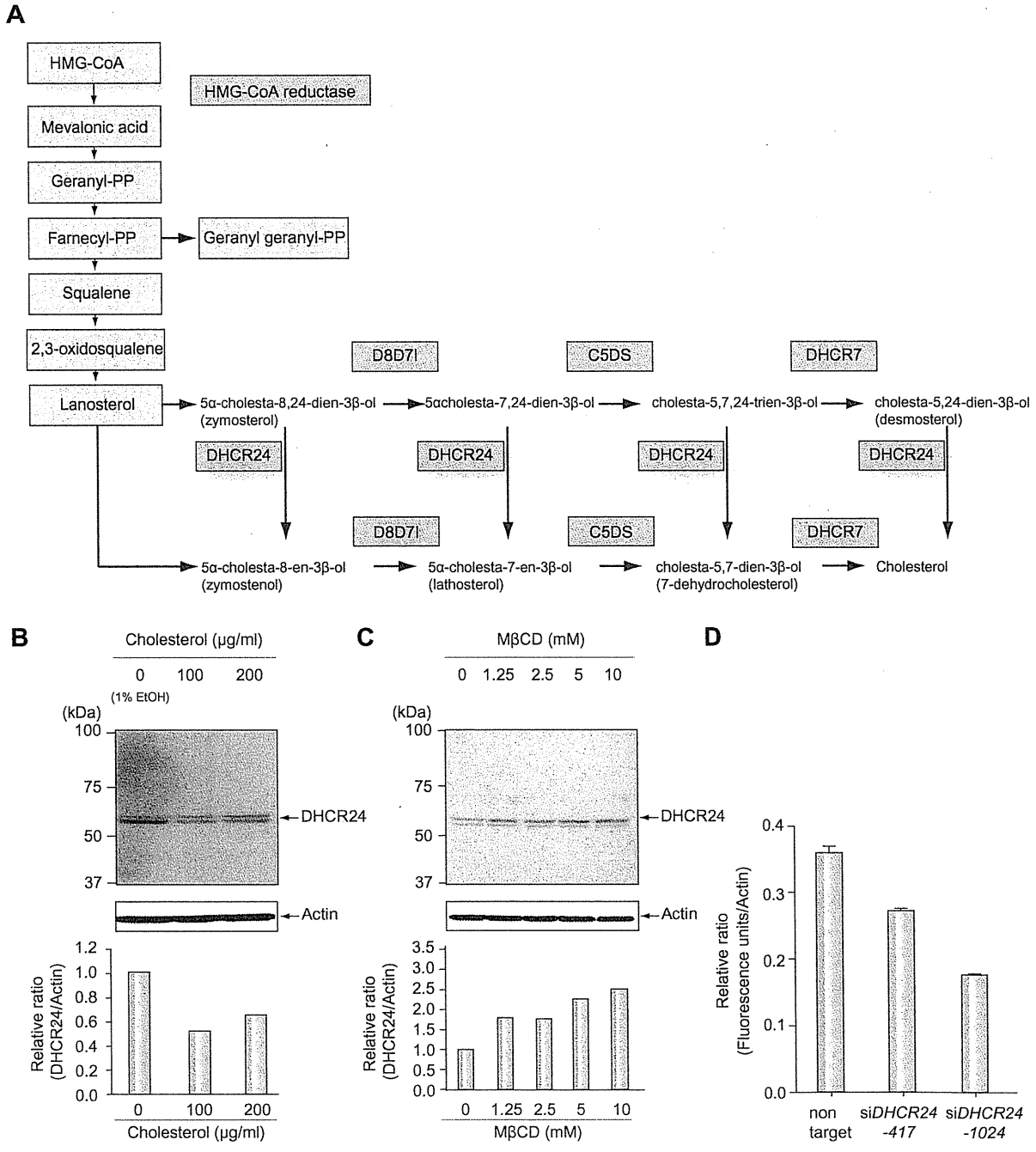

Fig. 3. The level of cholesterol and DHCR24 expression. (A) Cholesterol synthesis pathway, starting from HMG-CoA [26]. The abbreviations used are: D8D7I, 3β-hydroxysterol-delta(8)-delta(7)-isomerase; and C5DS, 3β-hydroxysterol-C^5-desaturase. (B) Cholesterol (0, 100, and 200 μg/ml) was added to HuH-7 cells, and, after 24 h, DHCR24 protein was detected by Western blot analysis using anti-DHCR24 MoAb and protein band intensity was measured and normalized to actin (lower panel). (C) HepG2 cells were treated with MβCD (0, 1.25, 2.5, 5, and 10 mM) for 30 min. After 72 h, these cells were harvested and examined by Western blot analysis with the anti-DHCR24 MoAb and relative intensity was measured as described in (B) (lower panel). (D) Cholesterol concentration in R6FLR-N cells was measured after treatment with non-targeting siRNA and *DHCR24* siRNA (417 and 1024). The cholesterol contents were measured by Amplex Red cholesterol assay, plotted based on fluorescence units and normalized to actin which was measured by Western blot analysis, and the relative ratio was then calculated. The data represent the mean of three experiments, and the bars indicate the SD values.

Research Article

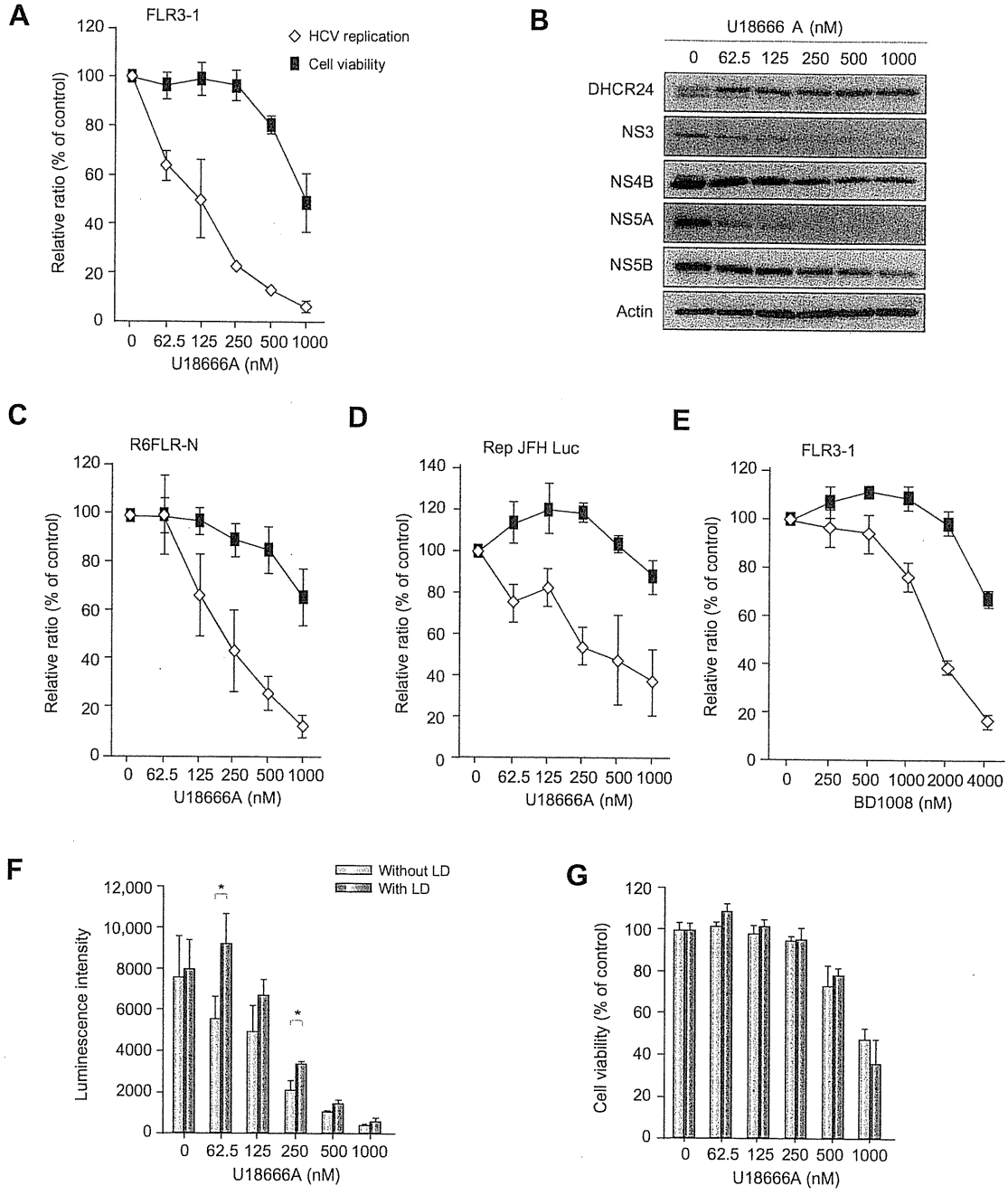

Fig. 4. Effect of U18666A on HCV replication. (A) Addition of U18666A to FLR3-1 cells and subsequent examination of HCV replication by the luciferase assay. Cell viability was measured by WST-8 assay. HCV replication and cell viability were measured 48 h after addition of U18666A. The bars indicate SD values. Open diamonds indicate the relative ratio of viral replication, and black squares indicate the cell viability in relation to untreated controls (A and C–E). (B) Treatment of FLR3-1 cells with U18666A decreased the expression of HCV proteins in a dose-dependent manner, as determined by Western blot analysis. (C and D) Effect of U18666A on HCV replication in other HCV replicon cells (C, R6FLR-N cells; D, Rep JFH Luc 3-13 cells). HCV replication and cell viability analyses were performed as described above. (E) The effect of the DHCR7 inhibitor BD1008 on HCV replicon cells (FLR3-1). Replication activity was examined by the luciferase assay, and cell viability was measured by the WST-8 assay. HCV replication and cell viability analyses were performed 48 h after the addition of U18666A. (F and G) FLR3-1 cells (5×10^3 cells/well) were treated with U18666A alone (light blue, or), low density lipoprotein (LDL) (final cholesterol concentration, 50 μg/ml), and U18666A (dark blue). HCV replication was determined by the luciferase assay 48 h later (F), and cell viability was measured by the WST-8 assay (G). *p <0.05 (two-tailed Student's t-test). The data represent the mean of three experiments, and the bars indicate SD values.